Molecular Biology of the Cell
Vol. 8, 871–895, May 1997

Pep7p Provides a Novel Protein that Functions in Vesicle-mediated Transport between the Yeast Golgi and Endosome

Gene C. Webb,*†‡ Jianqing Zhang,*§ Steven J. Garlow,*‖ Andreas Wesp,¶ Howard Riezman,¶ and Elizabeth W. Jones*†#

*Department of Biological Sciences and †The Center for Light Microscope Imaging and Biotechnology, Carnegie Mellon University, Pittsburgh, Pennsylvania 15213; and ¶Biozentrum of the University of Basel, CH-4056 Basel, Switzerland

Submitted November 1, 1996; Accepted February 26, 1997
Monitoring Editor: Randy Schekman

Saccharomyces cerevisiae pep7 mutants are defective in transport of soluble vacuolar hydrolases to the lysosome-like vacuole. *PEP7* is a nonessential gene that encodes a hydrophilic protein of 515 amino acids. A cysteine-rich tripartite motif in the N-terminal half of the polypeptide shows striking similarity to sequences found in many other eukaryotic proteins. Several of these proteins are thought to function in the vacuolar/lysosomal pathway. Mutations that change highly conserved cysteine residues in this motif lead to a loss of Pep7p function. Kinetic studies demonstrate that Pep7p function is required for the transport of the Golgi-precursors of the soluble hydrolases carboxypeptidase Y, proteinase A, and proteinase B to the endosome. Integral membrane hydrolase alkaline phosphatase is transported to the vacuole by a parallel intracellular pathway that does not require Pep7p function. *pep7* mutants accumulate a 40–60-nm vesicle population, suggesting that Pep7p functions in a vesicle consumption step in vesicle-mediated transport of soluble hydrolases to the endosome. Whereas *pep7* mutants demonstrate no defects in endocytic uptake at the plasma membrane, the mutants demonstrate defects in transport of receptor-mediated macromolecules through the endocytic pathway. Localization studies indicate that Pep7p is found both as a soluble cytoplasmic protein and associated with particulate fractions. We conclude that Pep7p functions as a novel regulator of vesicle docking and/or fusion at the endosome.

INTRODUCTION

A defining characteristic of all eukaryotic cells is the presence of distinct endomembrane organelles. These compartments allow a cell to perform often competing processes in separate environments suited to the particular requirements of each process (e.g., synthesis versus degradation). The presence of endomembrane organelles requires not only the formation and maintenance of the lipid components that delineate the different compartments but also the synthesis and targeting of proteins that serve either structural or enzymatic functions in the organelles. The yeast *Saccharomyces cerevisiae* has been used with great efficacy as a model system to dissect the eukaryotic secretory pathway and its functions in the synthesis and transport of proteins to both target organelles and the plasma membrane (Pryer *et al.*, 1992). It has been demonstrated that many of the same mechanisms are used in both unicellular eukaryotes and higher eukaryotes for entry into and progression through the secretory path-

‡ Present address: Howard Hughes Medical Institute, University of Chicago, Chicago IL 60637.
§ Present address: Department of Medicine, Division of Cell and Developmental Genetics, University of California, San Francisco, CA 94121.
‖ Present address: Department of Psychiatry and Behavioral Sciences, Emory University, Atlanta, GA 30322.
Corresponding author: Department of Biological Sciences, Carnegie Mellon University, 4400 Fifth Avenue, Pittsburgh, PA 15213.

© 1997 by The American Society for Cell Biology

way (reviewed in Ferro-Novick and Jahn, 1994; Rothman, 1994).

The yeast vacuole is thought to be analogous to the mammalian lysosome in that it is an acidic compartment (Preston *et al.*, 1989) that contains many of the cell's hydrolytic enzymes (reviewed in Klionsky *et al.*, 1990; Jones and Murdock, 1994; Van Den Hazel *et al.*, 1996) and is the destination of many endocytosed macromolecules (Riezman, 1993). Most vacuolar hydrolases are synthesized on the endoplasmic reticulum (ER) as inactive precursors, delivered to the vacuole via the secretory pathway, and activated by proteolytic processing upon delivery to the vacuole (reviewed in Jones *et al.*, 1989; Klionsky *et al.*, 1990; Jones, 1991b; Jones and Murdock, 1994; Van Den Hazel *et al.*, 1996). The inactive precursors synthesized on the ER proceed through the ER and Golgi complex along with proteins destined for secretion (reviewed in Klionsky *et al.*, 1990; Jones and Murdock, 1994; Van Den Hazel *et al.*, 1996). Transport of secreted proteins through the ER and Golgi complex has been demonstrated to proceed via vesicle-mediated transport (Rothman, 1994) and, subsequently, it has been shown that transport of vacuolar hydrolase precursors through the ER and Golgi complex also utilizes the same vesicle formation (Stevens *et al.*, 1982; Graham and Emr, 1991), docking (Stevens *et al.*, 1982; Banfield *et al.*, 1995), and fusion components (Stevens *et al.*, 1982; Klionsky *et al.*, 1988; Mechler *et al.*, 1988; Klionsky and Emr, 1989; Moehle *et al.*, 1989; Graham and Emr, 1991) as transport of secreted proteins. In a trans-Golgi network-like compartment (TGN) the vacuolar hydrolase precursors are sorted away from the secreted proteins and targeted to the vacuole (Graham and Emr, 1991). This conclusion is further supported by the observed involvement of yeast NSF (Sec18p) in transport through the vacuolar pathway (Graham and Emr, 1991). Recent evidence indicates that several vacuolar enzymes are transported from the TGN to an endosomal compartment and then subsequently on to the vacuole (Raymond *et al.*, 1992; Vida *et al.*, 1993; Piper *et al.*, 1995; Becherer *et al.*, 1996; Rieder *et al.*, 1996). Therefore, the yeast endosome is an intermediate compartment between a TGN-like organelle and the yeast lysosome (vacuole), and in this respect resembles higher eukaryotic endosomal compartments (reviewed in Kornfeld, 1987; Kornfeld and Mellman, 1989). Also, like higher eukaryotic endosomes, yeast endosomes are intermediate compartments between the plasma membrane and the vacuole in the endocytic pathway (Singer and Riezman, 1990; Davis *et al.*, 1993; Schimmoller and Riezman, 1993; Singer-Kruger *et al.*, 1993; Piper *et al.*, 1995; Rieder *et al.*, 1996).

Vesicle-mediated protein transport in the secretory pathways of eukaryotes has been shown to utilize a constellation of proteins that impart targeting specificity so that transport vesicles dock onto and fuse only with the appropriate target organelle (reviewed in Ferro-Novick and Jahn, 1994; Rothman, 1994). This complex of proteins has been designated the SNARE (SNAP receptor) complex. Docking specificity is thought to be effected by interaction between specific v-SNAREs and t-SNAREs on vesicle and target membranes, respectively.

Work in this laboratory and others has defined more than 40 complementation groups (*PEP* and *VPS*) that are required for either transport of vacuolar hydrolases to the vacuole and/or for formation of the vacuolar compartment. The *pep* mutants were isolated as deficient for carboxypeptidase Y (CPY) activity (Jones, 1977) and the *vps* mutants as secretors of vacuolar hydrolase proteins (Bankaitis *et al.*, 1986; Rothman and Stevens, 1986; Robinson *et al.*, 1988; Rothman *et al.*, 1989; Raymond *et al.*, 1992).

Analysis of the predicted *PEP* and *VPS* gene products revealed some with similarity to gene products found in SNARE complexes. These include Pep12p and Vps45p, which show sequence similarity to syntaxin, a t-SNARE (Becherer *et al.*, 1996), and Sec1p proteins, respectively (Cowles *et al.*, 1994; Piper *et al.*, 1994; Becherer *et al.*, 1996). Both Pep12p and Vps45p are thought to function in vesicle docking in transport between the TGN and endosome (Cowles *et al.*, 1994; Piper *et al.*, 1994). A comparison of the phenotypes of *pep12* and *vps45* mutants indeed suggests that they operate at the same step of transport (Raymond *et al.*, 1992; Cowles *et al.*, 1994; Piper *et al.*, 1994; Becherer *et al.*, 1996).

With the evidence that SNARE component homologues participate in transport between the yeast Golgi complex and the vacuole, it seems likely that this nonessential branch of the yeast secretory pathway can be exploited to investigate the basic eukaryotic phenomenon of vesicle-mediated transport. Although similarities are evident between TGN/endosome transport and the multiple steps in the secretory pathway, at least one difference is evident. The endosome receives cargo from at least two organelles (the TGN and plasma membrane; Piper *et al.*, 1995; Rieder *et al.*, 1996). This is unlike organelles in the secretory pathway, which are thought to receive cargo from only one upstream compartment. It is not clear what this difference might entail functionally.

This article describes the isolation and characterization of the *PEP7* gene and its encoded gene product. Mutations in *PEP7* lead to a block in trafficking and/or processing of not only CPY, but also protease A (PrA), protease B (PrB), and alkaline phosphatase (ALP). Additionally, *pep7* mutants show defects in transport through the endocytic pathway. Data presented here show that *PEP7* is a nonessential gene that encodes a 59-kDa protein found both as a peripheral membrane protein on the outside of a cytoplasmic compartment and as a soluble cytosolic protein. In strains lacking

Pep7p function, a 40–60-nm vesicle population accumulates, suggesting that Pep7p may function in a vesicle docking step of vesicle-mediated transport. The isolation of a temperature-sensitive allele is described and pulse-chase experiments with mutants carrying this allele are presented. Results from these experiments indicate that Pep7p is a unique protein that functions in vesicle-mediated transport of Golgi-precursor CPY, PrA, PrB, but not ALP from the TGN to the endosome.

MATERIALS AND METHODS

General Materials

Restriction enzymes were purchased from Boehringer Mannheim (Indianapolis, IN), New England Biolabs (Beverly, MA), or Promega Corporation (Madison, WI), T4 DNA ligase and Taq DNA polymerase were purchased from Boehringer Mannheim, and calf intestinal ALP was purchased from Promega Corporation (Madison, WI). All enzymes were used according to the manufacturer's instructions.

Media

YEPD and synthetic media for yeast cells were prepared as described previously (Woolford *et al.*, 1990). YEPD solid media with added ions were produced by making 100 ml of sterile YEPD minus the volume of sterile salt solution to be added (6 mM $ZnCl_2$: 1.2 ml of 250 mM $ZnCl_2$; 200 mM $CaCl_2$: 20 ml of 1 M $CaCl_2$; 200 mM $SrCl_2$: 20 ml of 1 M $SrCl_2$; 3 mM $MnCl_2$: 1.2 ml of 250 mM $MnCl_2$; 900 mM NaCl: 20 ml of 4.5 M NaCl). YPUADT is 1% yeast extract, 2% peptone (both Life Technologies, Pailsley, United Kingdom) 20 mg/l uracil, adenine, and tryptophan (E. Merck, Darmstadt, Germany), and 2% glucose. LB and M9 bacterial media have been described (Sambrook *et al.*, 1989). Ampicillin was purchased from Sigma Chemical Co. (St. Louis, MO) and used at 100 μg/ml.

General Yeast Methods

Standard procedures were used for all manipulations of yeast strains and have been described elsewhere (Sherman, 1991). Yeast transformations were carried out using a lithium acetate/dimethyl sulfoxide procedure (Hill *et al.*, 1991).

Overlay Assay for CPY Activity

Plate overlay assays for CPY activity were carried out as described previously (Jones, 1991a). Colonies exhibiting CPY activity stain pink to red (Pep^+), whereas colonies lacking this activity remain yellow to white (Pep^-).

Nucleic Acids Techniques

Molecular genetic techniques were generally those described in general laboratory manuals (Ausubel *et al.*, 1987; Sambrook *et al.*, 1989). Plasmid DNA minipreparations were made using the alkaline lysis method (Sambrook *et al.*, 1989). Yeast genomic DNA was prepared according to the method of Last *et al.* (1984). Plasmid shuttle from yeast to *Escherichia coli* was accomplished using the method of Hoffman and Winston (1987). PCR was carried out by standard methods in a DNA Thermal Cycler from Perkin Elmer-Cetus (Norwalk, CT; White *et al.*, 1989) using thermal-resistant DNA polymerase from Promega or Boehringer Mannheim with the manufacturer's buffers. Polymerase chain reaction (PCR) amplification of DNA from whole yeast cells was carried out by dispersing a freshly grown yeast colony (36 h at 30°C) into a standard PCR reaction.

Generation of pep Mutants

pep mutants were previously identified (Jones, 1977). Alleles *pep7–10*, *-12*, *-13*, *-14*, *-15*, and *-16* were isolated from parent strain BJ1983 as those colonies that lacked or exhibited reduced CPY activity as assayed by plate overlay assay (see above). *pep7–11*, from parent strain BJ863, was initially identified as *pep17–1* (Jones *et al.*, 1981). This mutant was repeatedly backcrossed into the S288c genetic background. Allele *pep7–17* was isolated in a mutant hunt for cells that could not acidify their vacuole as assayed by 6-carboxyfluorescein diacetate (6-CFDA) ratio staining (Preston *et al.*, 1992).

DNA Sequencing

Fragments of the original complementing library plasmid (pBJ3952) were subcloned into YCp50 and tested for the ability to complement the Pep^- phenotype of a *pep7::LEU2* deletion allele containing strain (BJ4000). In this way a minimal *PEP7* complementing 1.8-kb *Eco*RV/*Hin*cII fragment was determined (pBJ4928). This fragment was cloned into the *Sma*I site of vectors pTZ18U and pTZ19R (Genescribe-Z vectors, United States Biochemical, Cleveland, OH), yielding plasmids pBJ4640 and pBJ4639, respectively. A series of subclones was constructed, transformed into *E. coli* strain JM101, and single-stranded DNAs were prepared as templates for sequencing. The sequencing reactions were carried out using the Sequenase sequencing kit (United States Biochemical) and Genescribe-Z vector universal primer (Primer U) and reverse primer (Primer R). All were used according to the manufacturer's instructions. The minimal complementing fragment contained a single open reading frame (ORF) 1545 bp long. The sequence was deposited in GenBank, accession number U22070.

The nucleotide changes in the *pep7–10* through *pep7–17* mutant alleles were localized by gap repair and were cloned by generating PCR fragments directly from a fresh colony of the mutant strain (see Nucleic Acid Techniques) followed by cloning into pKB711 or YEp24. The mutant strains used were the following: BJ2329 (*pep7–10*), BJ2330 (*pep7–11*), BJ2194 (*pep7–12*), BJ2202 (*pep7–13*), BJ2212 (*pep7–14*), BJ2218 (*pep7–15*), BJ2231 (*pep7–16*), and BJ5124 (*pep7–17*). For all of the alleles, the region defined as carrying the mutation by gap repair was sequenced by double-stranded DNA sequencing (see below) to identify the mutation using *PEP7*-specific primers. To confirm that the identified mutation caused the observed Pep^- phenotype, the region containing a mutation was subcloned into a plasmid containing the *PEP7* gene and tested to confirm that the mutation found was unable to complement the Pep^- phenotype of yeast strain BJ4000. The reciprocal subcloning was also carried out to determine whether the observed mutation was the only one in the allele that would give a Pep^- phenotype.

Different *PEP7* constructs utilized in this study (introduced *Not*I restriction site and hemagglutinin (HA) epitope-tagged *PEP7*) were sequenced using double-stranded miniprepped DNA and primer PEP7 II (5′-GTGGAGATTCCGCGAATG-3′, located 21 nucleotides downstream of the *PEP7* ORF).

Polyclonal Antibody Production

Polyclonal rabbit antisera to a TrpE-Pep7p fusion protein were raised according to the procedure of Manolson *et al.* (1989). Rabbits were immunized using *E. coli*-derived protein from a *Eco*RI-*Sal*I fragment of *PEP7* in the pATH11 expression vector (yielding pBJ3960).

Antibody Purification

Pep7p polyclonal antisera were purified by blotting the antiserum against total proteins from a strain deleted for the *PEP7* gene, BJ4000, as described in the immunoblotting methods at a dilution of 1:200 in Tris-buffered saline + Tween 20 (9 g NaCl, 1.21 g Tris, pH 7.3, 0.5 ml Tween 20/1 l dH_2O). Those antibodies that did not bind were removed and stored at 4°C. Alternatively, whole undiluted

antiserum was incubated with 1% wt/vol acetone extracted proteins from BJ4000 on ice for 15 min followed by centrifugation at 10,000 × *g* for 15 min at 4°C.

Electron Microscopy

Cells subjected to electron microscopy were processed by a procedure described elsewhere (Banta *et al.*, 1988), with modifications. Cells were grown in 5 ml of YEPD to an OD_{600} of approximately 0.5. Cells were fixed for 2 h at 30°C by the addition of 3% glutaraldehyde, 5 mM $CaCl_2$ buffered with 100 mM sodium cacodylate, pH 6.8. Cells were collected by centrifugation and washed once in 100 mM Tris-HCl (pH 8.0), 25 mM dithiothreitol, 5 mM EDTA, and 1.2 M sorbitol. The cells were incubated in the same solution for 10 min at 30°C. The cells were then washed once in 0.1 M K_2HPO_4 (adjusted to pH 5.8 with citric acid) and 1.2 M sorbitol. The cells were resuspended in 0.5 ml of the same buffer. To this cell suspension was added 50 μl of β-glucuronidase type H-2 (114,000 U/ml, Sigma) and 2.5 mg of Zymolyase 20T (20,000 U/g, Seikagaku Corp., Tokyo, Japan). The cells were incubated for 2 h at 30°C to allow cell wall removal. After washing three times with 100 mM sodium cacodylate buffer containing 5 mM $CaCl_2$, the cells were postfixed for 30 min at room temperature in 1% OsO_4, 1% K-ferrocyanide, and 5 mM $CaCl_2$ buffered with 100 mM sodium cacodylate, pH 6.8. The samples were washed four times with dH_2O, resuspended for 5 min in 1% thiocarbohydrazide in dH_2O, washed four times with dH_2O, and fixed for 5 min in 1% aqueous OsO_4. The samples were washed four times with dH_2O and dehydrated in an EtOH series (50, 70, 80, 90, and 100%) followed by two washes with 100% propylene oxide. The samples were infiltrated in a (1:1) propylene oxide:LR White resin mixture for several hours, transferred to 100% LR White resin, and infiltrated overnight at room temperature. The next day, a fresh change of 100% LR White resin was added, and infiltration was extended for an additional 8 h. The resin was polymerized in gelatin capsules at 60°C for 24 h. Thin (80 nm) sections were cut using a DDK diamond knife on a Reichert-Jung Ultracut E. The sections were picked up on copper grids, stained with Reynolds lead citrate, viewed, and photographed on a Hitachi 7100 transmission electron microscope operated at an acceleration voltage of 50 keV.

6-CFDA Staining

Cells were labeled with the vital vacuolar stain 6-CFDA as described elsewhere (Preston *et al.*, 1989). The cells and filter were placed in an Eppendorf tube containing 100 μl of ice-cold MHKND buffer. The cells were then mounted onto microscope slides and viewed on a Zeiss fluorescent microscope, with excitation at 495 nm.

Lucifer Yellow Staining

The ability of the isogenic strains BJ5416 (*PEP7*), BJ8864 (*pep7Δ*), and BJ8865 (*end4Δ*) to carry out endocytosis was assayed by the ability of these strains to take up and deliver Lucifer yellow to the vacuole as described previously (Dulic *et al.*, 1991). The stained cells were visualized using a fluorescence microscope fitted with fluorescein isothiocyanate and Nomarski optics.

Pheromone Uptake and Degradation

^{35}S-labeled α-factor was prepared and isolated as described previously (Dulic *et al.*, 1991). Pheromone uptake was performed as described earlier (Dulic *et al.*, 1991) with the following changes. Cultures were grown in YPUADT to 0.5–1 × 10^7 cells/ml and harvested by centrifugation at 2000 rpm for 5 min in a general laboratory centrifuge (GLC, Sorvall) in 50-ml Falcon tubes. Cells were resuspended to 3 × 10^8 cells/ml in YPUADT and preincubated for 10 min at the indicated temperature on a rotary-aquashaker (Kuhner, Birsfelden, Switzerland) before ^{35}S-labeled α-factor was added. Cells were harvested at various time points by diluting them 100-fold into ice-cold pH 1 (50 mM sodium citrate) or pH 6 (50 mM potassium phosphate) buffer. pH 6 samples were filtered immediately onto GF/C filters (Whatman, Maidstone, United Kingdom) on a vacuum pump, whereas pH 1 samples were kept on ice for 20 min prior to filtering. Filters were washed with the respective ice-cold buffer, transferred to 20-ml screw-cap polyethylene scintillation vials (Packard, Meriden, CT), and dried at 80°C for 15 min before adding 5 ml of emulsifier-safe scintillation cocktail (Packard) and counting each sample in a beta counter (1900 TR, Packard). Percentage of internalized α-factor was determined as 100 × cpm (pH 1)/cpm (pH6). Internalization assays were performed twice.

Pheromone degradation assays were performed as follows. Cells were grown in YPUADT overnight at 24°C on a rotary shaker to 0.9–1.1 × 10^7 cells/ml. Cells (5 × 10^8) were harvested by centrifugation at 3000 rpm for 5 min in a GLC (Sorvall) in 50-ml Falcon tubes and washed once with 20 ml of ice-cold YPUADT. Cells were resuspended in 1.6 ml of ice-cold YPUADT, and ^{35}S-labeled α-factor was added and incubation was continued for 60 min on ice. Unbound α-factor was removed by pelleting cells in a GLC. Cells were then resuspended in 1.6 ml of prewarmed YPUADT at 24 and 37°C, respectively. Aliquots (0.2 ml) were harvested immediately (t = 0) and diluted 100-fold into ice-cold pH 1 (50 mM sodium citrate) or pH 6 (50 mM potassium phosphate) buffer. After t = 7.5, 15, 30, 60, and 90 min, 0.2-ml aliquots were harvested into ice-cold pH 1 buffer as described above. Cells were then filtered through HA 0.45-μm Millipore filters which were presoaked in 1% bovine serum albumin (BSA, Sigma). Filters were washed once with pH 6 buffer and transferred to 2-ml Eppendorf tubes. Cells were washed off the filters with 1 ml of pH 6 buffer and pelleted in a microfuge at 10,000 rpm for 2 min. Cells were then resuspended in 0.2 ml of extraction buffer (40% methanol, 0.25% trifluoroacetic acid (TFA), 0.1% 2-mercaptoethanol, 0.6% HOAc) on ice. Radiolabeled α-factor was extracted by four consecutive cycles of freeze-thawing in liquid nitrogen with vigorous vortexing in between. Unbroken cells were removed by centrifugation and 0.12 ml of the supernatant was loaded onto TLC plates (silica gel 60, Merck, Darmstadt, Germany). The plates were run for 12 h in 220 ml of buffer (100 ml butanol, 50 ml propionic acid, 70 ml water), dried, sprayed with En^{3}Hancespray (New England Nuclear, Boston, MA) and exposed to Kodak XAR-5 film at −80°C for 3 d.

Radiolabeling Spheroplasts

Radiolabeling of spheroplasts was carried out by a combination of protocols as described elsewhere (Robinson *et al.*, 1988; Rothblatt and Schekman, 1989; Herman *et al.*, 1991). In experiments where vacuolar hydrolases were immunoprecipitated from medium (external) and spheroplast (internal) fractions, cells were grown to early log phase in Wickerham's minimal proline medium containing 200 μM $MgSO_4$ and 0.2% yeast extract. Two to four OD_{600} units of cells/sample for each gel lane were collected by centrifugation. The cells were resuspended in prewarmed 0.1 M Tris sulfate (pH 9.4)/10 mM dithiothreitol and incubated for 5 min at 30°C. Cells were collected and resuspended in prewarmed spheroplasting medium (Wickerham's as above + 0.7 M sorbitol, pH 7.4). Thirty units of lyticase (Sigma)/OD_{600} were added and the cells were incubated for 30 min at 30°C with gentle agitation. Spheroplasts were pelleted at approximately 750 × *g* for 5 min, washed once in prewarmed spheroplasting medium, and resuspended in prewarmed labeling medium (same as spheroplasting medium made to 1 mg/ml BSA and only 20 μM $MgSO_4$). Spheroplasts were allowed to recover for 5 min at 30°C before 50 μCi of Trans^{35}S-labeling reagent (ICN Radiochemicals, Irvine, CA)/OD_{600} units spheroplasts were added. Spheroplasts were incubated for 20 min at 30°C with gentle agitation. A chase was initiated by adding unlabeled methionine and cysteine each to 25 mM and yeast extract to 0.4%, and the incubation was continued for 30 min. The cultures were transferred to Eppendorf tubes and spun for 20 s to separate the medium (containing the external, secreted hydrolase fraction) from the cell pellet (containing the internal, cell-associated hydrolase fraction). The medium was

made 5% trichloroacetic acid (TCA) by the addition of 100% TCA, and the cell pellet was resuspended in 5% TCA. All samples were incubated for 20 min on ice. The samples were pelleted and the pellets were washed twice with ice-cold acetone, dried at room temperature, and resuspended in 600 μl of suspension buffer [50 mM Tris (pH 7.5)/1 mM EDTA/1% SDS]. Glass beads were added and the samples were vortexed for 1 min at room temperature, incubated for 5 min at 105°C, vortexed again for 1 min, and let cool to room temperature. The fractions were separated into four equal aliquots, from which CPY, PrA, PrB, and ALP were immunoprecipitated (see Immunoprecipitation). Affinity-purified CPY antibody was a kind gift from Tom Stevens. Affinity-purified ALP antibodies were a kind gift from Scott Emr. Affinity-purified PrA and PrB antibodies were described elsewhere (Moehle *et al.*, 1989; Woolford *et al.*, 1990). Labeling of temperature-sensitive strains was carried out essentially as described above, but with the following modifications: 1) all steps of spheroplast formation were done at room temperature; 2) spheroplasts were preincubated at restrictive temperatures for 5 to 10 min prior to initiating; and 3) labeling was carried out for 5 min at temperatures indicated in the figure legends with 50 μCi of Trans^{35}S-labeling reagent/OD_{600} units spheroplasts, followed by a 45-min chase.

In experiments where hydrolases were immunoprecipitated from whole-cell fractions (external and internal combined), cells were grown to early log phase, and 2–4 OD_{600} units of cells/sample for each lane were collected and washed once with labeling medium (as above, but lacking 0.7 M sorbitol). Cells were then labeled as described above for spheroplasts. Following a chase incubation, the labeled culture was brought to 10% TCA by the addition of 100% TCA and incubated on ice for 20 min. The precipitated culture was then treated as described above.

Protease K Protection Assay and Salt Extraction

For protease K protection assays and salt extraction experiments, radiolabeled extracts were produced as described elsewhere (Rothblatt and Schekman, 1989). Briefly, strain BJ7995 was grown in low-sulfate Wickerham's medium [200 mM $(NH_4)_2SO_4$] to early log phase (OD_{600} = 0.5). Viable spheroplasts were produced as described above using osmotically supported (0.7 M sorbitol) low-sulfate Wickerham's medium. Spheroplasts were labeled by the addition of $Na_2{}^{35}SO_4$ (ICN Radiochemicals) to 170 μCi/OD_{600} and incubation for 60 min at 30°C. Labeling was stopped by the addition of 0.01 volume of 100 mM $(NH_4)_2SO_4$/0.3% cysteine/0.4% methionine followed by a chase incubation of 20 min at 30°C. Cell extracts with intact membrane compartments were produced by centrifugation of the spheroplasts onto a 1.9 M sorbitol/50 mM Tris (pH 7.5) cushion, resuspension in lysis buffer [27–40 ml/OD_{600}; 0.3 M mannitol/0.1 M KCl/50 mM Tris (pH 7.5)/1 mM EGTA/10 mM Na_2N_3/1 μM phenylmethylsulfonyl fluoride/0.1 μM leupeptin], and homogenization (three times for 1 min at approximately 60 rpm/min with 1 min in between on ice) in a 4-ml homogenizer fitted with a Teflon pestle (Kontes Glass Co., Vineland, NJ). Unlysed cells were removed by centrifugation for 4 min at 650 × *g* at 4°C.

For protease K protection assays, a total of 21 OD_{600} spheroplasts were labeled as described in the preceding paragraph and resuspended in 820 μl of lysis buffer prior to homogenization. The cell extract was divided into three equal aliquots and treated with or without protease K (0.3 mg/ml) and Triton X-100 (0.4%) for 15 min at 4°C. The reaction was stopped by the addition of TCA to 20%. The precipitated protein was collected by centrifugation, washed once with ice-cold acetone, dried, and resuspended in 200 μl of suspension buffer [50 mM Tris (pH 7.5)/1 mM EDTA/1% SDS] by incubating for 5 min at 95°C. Pep7::HAp was immunoprecipitated as described below with monoclonal antibodies directed against the HA epitope tag (clone 12CA5, Berkeley Antibody Co., Richmond, CA). As a control for organelle membrane integrity, ALP was immunoprecipitated from the same extracts.

For salt extraction studies of Pep7::HAp, radiolabeled extract was produced as described above from a total of 28 OD_{600} spheroplasts (in 1 ml of lysis buffer). The cell extract was divided into three equal aliquots and treated with an equal volume of one of the following for 10 min on ice: 2 M NaCl in lysis buffer, 10 M urea in lysis buffer, or unmodified lysis buffer. The samples were loaded into Beckman 13 × 51-mm TLA100 tubes and centrifuged in a Beckman bench top ultracentrifuge for 60 min at 103,000 × *g* (50,000 rpm) at 4°C. Supernatants were removed and 100% TCA was added to them to a final concentration of 10%. The pellets were resuspended in 10% TCA. Both were incubated on ice for 20 min and treated as described above.

Immunoprecipitation

Immunoprecipitations were carried out as described elsewhere (Rothblatt and Schekman, 1989). Because antigens were serially precipitated, antigens were removed from the first antigen/antibody complex by the addition of 200 μl of 1% SDS/50 mM Tris (pH 7.5) and heating to 105°C for 5 min. The supernatant was removed to a fresh tube, and immunoprecipitation with the same antibody was carried out with the addition of BSA at a final concentration of 150 μg/ml as carrier protein. Following the final wash in detergent-free wash buffer, the precipitates were resuspended in 25 μl of denaturation (Laemmli) buffer (1% SDS/1% β-mercaptoethanol/10% glycerol, 50 mM Tris, pH 6.8, 0.1% bromphenol blue; Laemmli, 1970), heated to 105°C for 5 min, cooled to room temperature, and the supernatant loaded on SDS-denaturing polyacrylamide gels (see figure legends for percentage of acrylamide in each gel).

Autoradiography

Polyacrylamide gels were submerged in Resolution autoradiography enhancer (EM Corp., Chestnut Hill, MA) for 30 min followed by a 45-min incubation in cold dH_2O, all with gentle mixing. The gels were then dried for 45 min at 65–70°C under vacuum and then exposed to film (Kodak X-OMAT AR or BIOMAX MR). Quantitation of autoradiographs was carried out on an Ambis 4000 optical imager using core software version 4.0.

Generation of a *pep7^{ts}* Allele

A *pep7^{ts}* allele was generated by hydroxylamine mutagenesis of plasmid DNA followed by transformation directly into yeast (Rose and Fink, 1987). A *ScaI*/*SalI* fragment containing *PEP7* cloned into pRS316 was used as the plasmid DNA and BJ8081 (*MAT***a** *ura3–52 leu2 pep7::LEU2*) was used as the recipient yeast strain. Seventy micrograms of Qiagen column (Qiagen Inc., Chatsworth, CA) prepared plasmid DNA was dissolved in 3.5 ml of a freshly made ice-cold hydroxylamine solution: 0.09 g NaOH/0.35 g hydroxylamine hydrochloride (Sigma MO)/5 ml ice-cold sterile dH_20. The DNA was mutagenized for 20 h at 42°C. The reaction was terminated by the addition of 87.5 μl of 4 M NaCl, 350 μg of BSA, and 7 ml of cold ethanol. The DNA was pelleted, resuspended in 700 μl dH_20, reprecipitated with sodium acetate and ethanol, pelleted again, and dried. The DNA was dissolved in a small volume of dH_2O and transformed into yeast strain BJ8081 using the LiAc/DMSO protocol. DNA was also transformed into *E. coli* (BJ7253: *pyrF::TN5-sup trp-am lac-am*) to test the mutagenesis frequency: 1 of 34 amp^r colonies (2.9%) was unable to grow on M9 plates, indicating a mutation in the plasmid-borne *URA3* sequence. Transformed yeast cells were plated onto 42 C-Ura plates, yielding approximately 18,000 colonies total. These colonies were replica plated onto two YEPD/6 mM $ZnCl_2$ plates and incubated at 23°C or 37°C. Those colonies that grew at 23°C but not at 37°C were picked, phenotypes retested, plasmids shuttled through *E. coli*, and phenotypes again tested. One plasmid, pBJ8234, gave the expected results in all of these assays. The mutation was localized by subcloning and double-strand sequencing (see sequencing methods in this section) and the plasmid was found to contain a single nucleotide change (cytosine-756 to guanine) that changes Cys-252 to Trp.

Epitope Tagging Pep7p

To epitope tag Pep7p with a triple HA tag, a *Not*I restriction site was introduced between the last sense codon and the stop codon of *PEP7* by PCR. PCR was carried out using primer PEP7 E (5'-CCGCA-CAGTAGTACC-3', matching nucleotides 344–359 of the *PEP7* ORF) and primer PEP7 3' *Not*I (5'-TTA GCG GCC GCC ATT AAA CCC ATG GTC ACC-3', matching nucleotides 1545–1530 of the *PEP7* ORF). The resulting PCR fragment of *PEP7* was reintroduced to the complete ORF by "polishing" the ends of the resulting PCR product with Klenow enzyme (Boehringer Mannheim) and cutting with *Cla*I. A complete *PEP7* ORF (*Sca*I/*Sal*I fragment) in vector pKB711X (Becherer *et al.*, 1996) was cut with *Pac*I, blunted with mung bean nuclease (Boehringer Mannheim), and cut with *Cla*I. The polished and cut PCR product was ligated into this DNA and transformed into *E. coli* strain LM1035. The resulting construct (pBJ7687) was sequenced as described in DNA Sequencing. With the completion of these manipulations, the 3' end of *PEP7* contains the following sequence: GGT GAC CAT GGG TTT AAT GGC GGC CGC TAA TAA GAC ATA. This construct was cut with *Not*I and a *Not*I fragment encoding a triple influenza HA epitope tag (kind gift from Bruce Futcher, Cold Spring Harbor Laboratory, Cold Spring Harbor, NY and Susan Michaelis, Johns Hopkins University, Baltimore, MD) was inserted by ligation. The insertion orientation was monitored by restriction digest. The resulting construct (pBJ7720) was digested with *Bst*EII and *Sac*II, and the resulting fragment was ligated into the *Bst*EII/*Sac*II site of pBJ4272 (pBJ4272 = 3.8-kb *Sal*I genomic *PEP7* fragment in the *Sal*I site of Yep24), yielding the plasmid pBJ7686. The-3.8 kb *PEP7::HA Sal*I fragment from pBJ7686 was used to transplace the *pep7*Δ*::LEU2* allele in the yeast strain BJ4000 by single-step gene transplacement yielding yeast strain BJ7995.

Cell Fractionation by Differential Centrifugation

Fractionation by differential centrifugation was carried out as described previously (Becherer *et al.*, 1996) using strain BJ7995.

Preparation of Yeast Nuclei

Nuclei were prepared as described previously (Kalinich and Douglas, 1989) using strain BJ1983. To be able to load sufficient amounts of proteins onto denaturing polyacrylamide gels, preparations were TCA precipitated and resuspended in Laemmli buffer (1% SDS/1% β-mercaptoethanol/10% glycerol, 50 mM Tris, pH 6.8) at appropriate concentrations.

Buoyant Density Preparation of Vacuolar Pathway Compartments

Buoyant density "floats" were prepared as described previously for vacuole preparations (Woolford *et al.*, 1990) using strain BJ1983.

Immunoblots

Protein extracts were subjected to SDS-PAGE (Laemmli, 1970). For Pep7p, RNA polymerase II, Vph1p, Kex2p, and CPY detection, extracts were separated on 10% polyacrylamide gels. PrA was separated on 12% gels. Immunoblotting was carried out as described elsewhere (Woolford *et al.*, 1990). RNA polymerase II antibodies were a kind gift from Sha-Mei Liao, Kex2p antibodies were a kind gift from Robert Fuller. Pep7p immune complexes were detected using a Vectastain avidin/biotin enhancement kit (Vector Laboratories, Burlingame CA) whereas all others were detected using secondary antibodies conjugated to horseradish peroxidase (Bio-Rad Laboratories, Richmond, CA). Immunoblots were incubated in 100 ml phosphate-buffered saline/0.06% H_2O_2, to which was added 60 mg of 4-chloro-1-naphthol (Sigma) in 20 ml of acetone-free methanol to detect horseradish peroxidase activity.

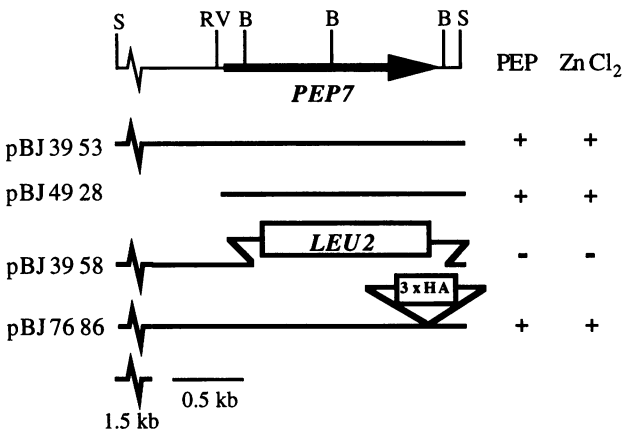

Figure 1. Characterization, disruption, and epitope tagging of the *PEP7* locus. The restriction map of complementing clone pBJ3953 (3.8-kb *Sal*I fragment) and smallest complementing fragment in pBJ4928 (1.8-kb *Eco*RV/*Sal*I fragment) are shown with the 1.545-kb *PEP7* ORF indicated with the solid arrow. The nucleotides from +165 (+1 is the A of the ATG) to +1617 were deleted and a *Bgl*II fragment bearing *LEU2* was inserted yielding plasmid pBJ3958. A triple HA epitope tag was inserted between the last sense codon and the stop codon yielding plasmid pBJ7686. Both the Pep phenotype and growth phenotype on YEPD containing 4 mM $ZnCl_2$ are indicated to the right. S, *Sal*I; RV, *Eco*RV; B, *Bgl*II; and 3×HA, triple HA epitope tag.

RESULTS

Identification and Cloning of PEP7

The *PEP7* gene was cloned from a YCp50 genomic library (supplied by M. Rose) by complementation of the CPY deficiency of a *pep7* mutant (Jones, 1977). Eighteen Pep^+ transformants were identified among 6800 Ura^+ transformants obtained by transformation of strain BJ2406 (*MAT***a** *ura3–52 leu2 trp1 pep7–11*; see Tables 1 and 2 for strains and plasmids). Five identical plasmids were identified after shuttling through *E. coli*. The plasmid, pBJ3952, contained approximately 10 kb of insert DNA. An internal 3.8-kb *Sal*I fragment was found to be able to fully complement the Pep^- phenotype (pBJ3953; Figure 1). To verify that this fragment contained the *PEP7* locus, the fragment was cloned into YIp5 (plasmid pBJ3954) and, after cleavage within the insert by *Hpa*I, used to direct the integration of the plasmid into strain BJ2406. When a Ura^+-Pep^+ integrant was crossed to wild-type *PEP7* strains, meiotic analysis of the resulting diploids gave 47 tetrads that all segregated 4:0 Pep^+:Pep^-, indicating that the 3.8-kb *Sal*I fragment contained the wild-type *PEP7* locus.

A minimal complementing 1.8-kb *Eco*RV/*Sal*I DNA fragment (pBJ4928; Figure 1) was cloned into sequencing vectors and sequenced. A 1545-bp ORF was found that encodes a predicted polypeptide 515 amino acids long and that is hydrophilic (isoelectric point of pH 8.4; Figure 2A). No signal sequence or hydrophobic

```
1    MDLENVSCPICLRKFDNLQALNAHLDVEHGFNDN

                                    -10 *
35   EDSLGSNDSRLVNGKQKKARSVDSSAQKLKRSHW
       T                          Q

69   EKFKKGKSCCHTCGRTLNNNIGAINCRKCGKLYC

103  RRHLPNMIKLNLSAQYDPRNGKWYNCCHDCFVTK
               P

137  PGYNDYGEVIDLTPEFFKVRNIKREDKNLRLLQL
     L

171  ENRFVRLVDGLITLYNTYSRSIIHNLKMNSEMSK

205  LERTVTPWRDDRSVLFCNICSEPFGLLLRKHHCR
                   G
      Y -12,-15    W -20
239  LCGMVVCDDANRNCSNEISIGYLMSAASDLPFEY

       * -13      -14 Y  Y -11
273  NIQKDDLLHIPISIRLCSHCIDMLFIGRKFNKDV

                      * -16
307  RMPLSGIFAKYDSMQNISKVIDSLLPIFEDSLNS

341  LKVETAKDSENTLDPKNLNDLARLRHKLLNSFNL

           * -17
375  YNTLTRQLLSVEPQSHLERQLQNSIKIASAAYIN

409  EKILPLKSLPAILNPEGHKTNEDGQKAEPEVKKL

443  SQLMIENLTIKEVKELREELMVLKEQSYLIESTI

477  QDYKKQRRLEEIVTLNKNLEELHSRIHTVQSKLG

511  DHGFN*
```

Figure 2. Predicted amino acid sequence of the *PEP7* gene product and identified mutations. The predicted amino acid sequence of the 515 residue polypeptide encoded by *PEP7* (GenBank accession number U22070) is shown. Changes in the amino acid sequence brought about by mutations that lead to a mutant phenotype are shown in bold above the wild-type sequence. The allele numbers are located to the right or left of the encoded change. Nonsense mutations are indicated by an asterisk. Mutations that do not lead to a mutant phenotype are indicated below the wild-type sequence in plain text. Sequence motifs are underlined.

domain that could serve as a transmembrane domain was predicted by computer analysis. There are several cysteine-rich sequences in the amino-terminal half of the polypeptide that show varying degrees of similarity to motifs found in other proteins. The most N-terminal of these (amino acids 6–29) shows similarity to the zinc finger repeats found in transcription factor TFIIIA of *Xenopus laevis* (Figures 2 and 3A; Berg, 1990). The cysteine-rich region found between amino acids 212–294 shows striking similarity to a tripartite cysteine-rich motif found in several eukaryotic proteins and uncharacterized ORFs (Figure 3B). These include regions of *FAB1* and *VPS27*, genes also thought to be involved in vacuolar function in yeast (Figure 3B; Piper *et al.*, 1995; Yamamoto *et al.*, 1995), as well as two additional uncharacterized ORFs in yeast (Figure 3). The order of the three parts of the motif is strictly conserved among the various proteins and ORFs, while some variability in the spacing of the three elements is observed. Furthermore, the location of the tripartite motif within the polypeptides varies among the proteins. Lysine/arginine-rich sequences located between amino acids 49–54, 62–65, and 70–75 show similarity to nuclear localization sequences (Figure 3C; Robbins *et al.*, 1991; Gorlich *et al.*, 1995). The *PEP7* sequence was deposited into GenBank, and accession number U22070 was assigned. While this work was in progress the *PEP7* locus was recloned and additionally designated *VAC1* (Weisman and Wickner, 1992). Moreover, complementation analysis between the PEP and VPS complementation groups revealed that *PEP7* and *VPS19* are allelic. Because mutations at this locus were first reported as *pep7* mutations (Jones, 1977), and the locus was mapped and is listed in the *S. cerevisiae* genome database as *PEP7*, we will use the *PEP7* designation.

A deletion of the *PEP7* locus was constructed by replacing a 1.4-kb *Bgl*II fragment of the *PEP7* ORF in plasmid pBJ3954 with a 3.0-kb *Bgl*II fragment from YEp213 containing the selectable marker *LEU2* (yielding plasmid pBJ3958; Figure 1). This construct removes nucleotides 165-1545 of the *PEP7* ORF plus 72 nucleotides downstream of the stop codon. This construct, when digested with *Sal*I, and transplaced into the genome of a diploid homozygous *PEP7 leu2*, directed the removal of one wild-type *PEP7* gene. Sporulation of the heterozygous diploid produced meiotic segregants in the ratio of 2 Pep^+ Leu^-::2 Pep^- Leu^+ for all 65 tetrads analyzed, as expected.

The mutations in the *PEP7* gene in the *pep7–10* through *pep7–17* mutants were sequenced; the changes are indicated above the sequence in Figure 2. Mutations recovered that did not affect *PEP7* function are indicated below the wild-type sequence. Interestingly, all missense alleles recovered (*pep7–11*, *-12*, *-14*, and *-15*, and including the *pep7–20 ts* allele) changed cysteine residues in the highly conserved C8 tripartite

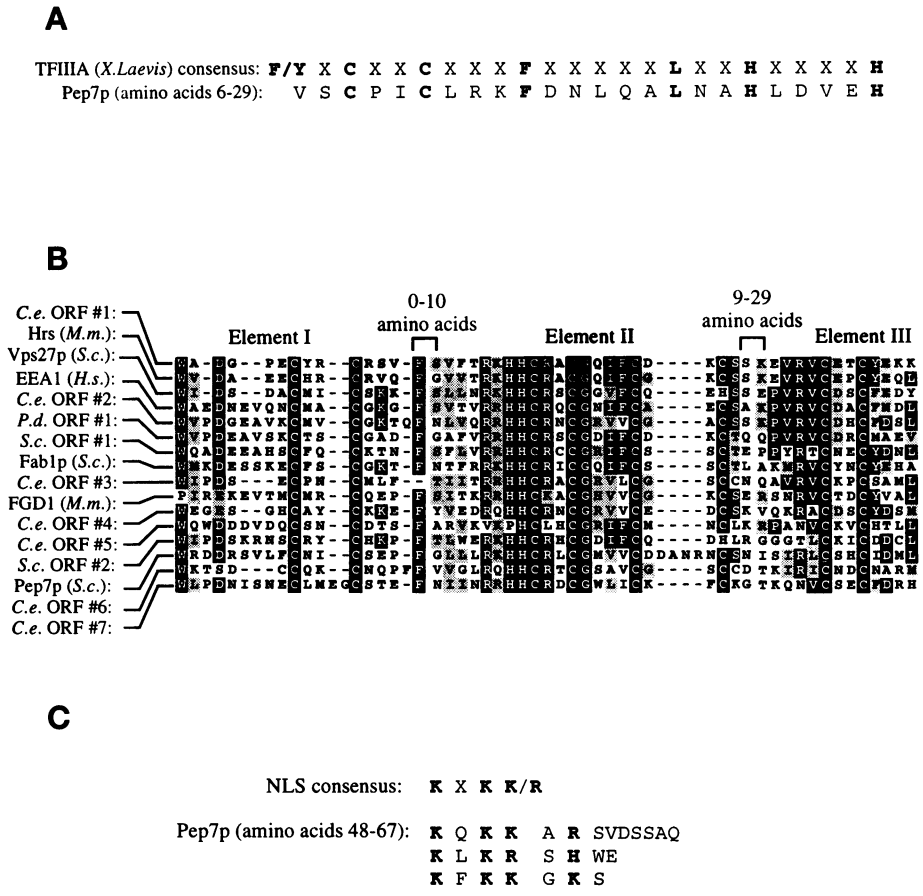

Figure 3. Sequence motifs found in the *PEP7* gene product. (A) Pep7p amino acids 6–29 show sequence similarity to the zinc finger repeat motif found in the *X. laevis* transcription factor TFIIIA. (B) Pep7p amino acids 212–294 show striking similarity to a tripartite cysteine-rich motif found in several other eukaryotic proteins and putative ORFs. The entries are identified as: C.e. ORF 1 from *Caenorhabditis elegans* (NCBI accession number 1326382) amino acids 193–252; Hrs from *Mus musculus* (NCBI accession number 1089781) amino acids 160–219; Vps27p from *S. cerevisiae* (NCBI accession number 1353233) amino acids 170–230; EEA1 from *Homo sapiens* (NCBI accession number 1016368) amino acids 1348–1408; C.e., ORF 2 from *C. elegans* (NCBI accession number 732235) amino acids 149–212; P.d. ORF 1 from *Phoenix dactylifera* (NCBI accession number 1246823) amino acids 215–277; S.c. ORF 1 from *S. cerevisiae* (NCBI accession number 849227) amino acids 14–87; Fab1p from *S. cerevisiae* (NCBI accession number 462047) amino acids 237–297; C.e. ORF 3 from *C. elegans* (NCBI accession number 746516) amino acids 538–600; FGD1 from *M. musculus* (NCBI accession number 722343) amino acids 726–788; C.e. ORF 4 from *C. elegans* (NCBI accession number 100859) amino acids 790–855; C.e. ORF 5 from *C. elegans* (NCBI accession number 529701) amino acids 341–401; S.c. ORF 2 from *S. cerevisiae* (NCBI accession number 1322491) amino acids 449–513; and C.e. ORF 6 from *C. elegans* (NCBI accession number 642176) amino acids 285–346. (C) Pep7p amino acids 48–67 show sequence similarity to nuclear localization sequences in viral large T antigen.

motif, and therefore, this motif is essential for Pep7p function.

pep7 Mutants Contain a Vacuole with an Abnormal Morphology and Accumulate a Vesicle Population in the Cytoplasm

Electron microscopy was used to analyze the ultrastructural defects brought about by the loss of *PEP7* function. Although *S. cerevisiae* lacks many of the visual cytoplasmic landmarks of higher eukaryotic cells, the vacuole is usually a prominent feature of the yeast cell and therefore gross perturbations that affect the vacuole are easily detectable by several microscopic techniques. In electron micrographs stained to highlight the vacuole in cells, a wild-type strain presents several (three to five) darkly staining vacuoles (Figure 4A). As demonstrated in this profile, the vacuole is partitioned to the developing bud as "streaming" of some of the vacuole fragments through the bud neck during the cell cycle. A strain deleted for *PEP7* shows a strikingly different profile. They contain a single large vacuole-like compartment (Figure 4D). Furthermore, as noted by others, neither this single large vacuole nor fragments of it are distributed to the bud as the cell divides (Weisman and Wickner, 1992). The fact that each cell ultimately acquires a single large vacuolar compartment despite not inheriting a vacuole from the mother cell suggests that strains lacking *PEP7* function are still capable of forming a vacuole de novo.

These observations on the vacuole morphology phenotype of *pep7* mutants were confirmed by fluorescence and differential interference contrast (DIC) mi-

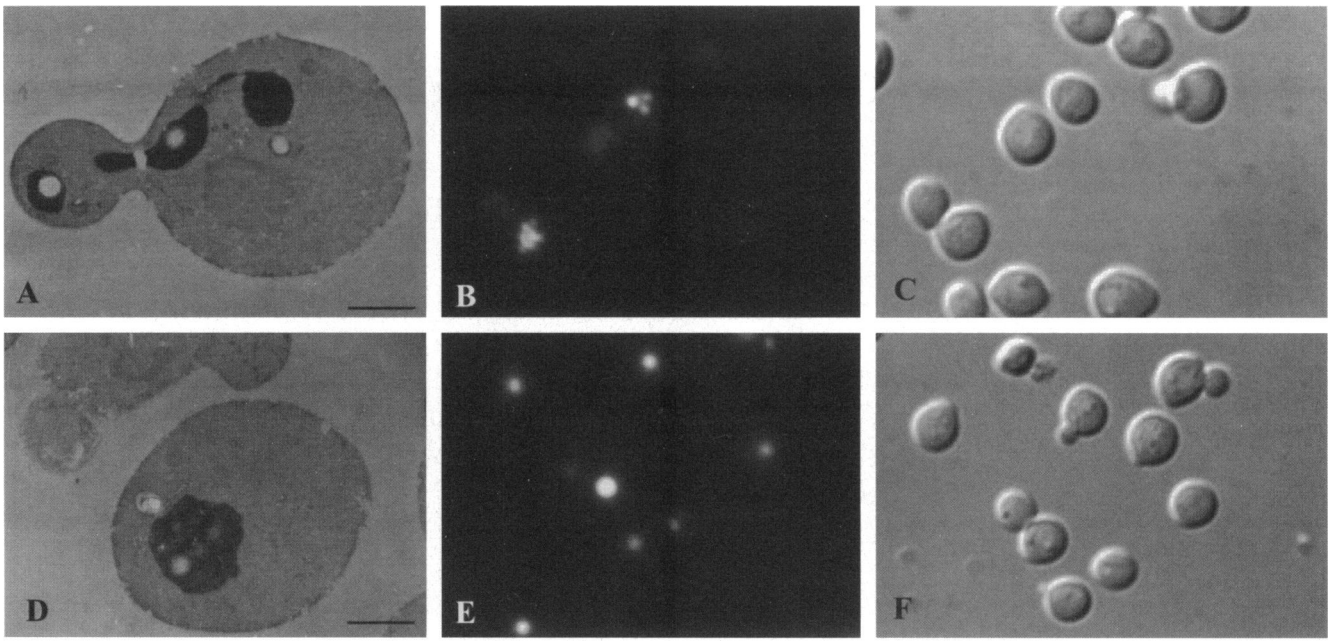

Figure 4. Morphology of the *pep7*Δ mutant strain. A–C are strain BJ2665 (*PEP7*). D–F are strain BJ8081 (*pep7*Δ*::LEU2*). (A and D), cells were prepared and stained for electron microscopy as described in MATERIALS AND METHODS. The vacuoles stain dark in these preparations. Bars, 1 μm. (B and E), cells were labeled with vital vacuolar stain 6-CFDA as described in MATERIALS AND METHODS. (C and F), Nomarski images of the same fields of cells shown in B and E, respectively.

croscopy using the vital dye 6-CFDA; free 6-carboxyfluorescein (6-CF) becomes trapped in the vacuole as a charged fluorescent molecule (Preston *et al.*, 1992). In these preparations, a wild-type strain contains multiple vacuolar compartments that correspond to cytoplasmic depressions seen in the DIC images (Figure 4, B and C). Again, as was seen in the electron microscopic profiles, cells of the *pep7* mutant strain contain a single large, very round vacuolar compartment as demonstrated by both 6-CF staining and DIC profiles (Figure 4, E and F). Because the fluorescence of 6-CF is pH dependent (Preston *et al.*, 1989), these and previous studies with 6-CFDA revealed that *pep7* strains contain vacuoles that are neutral in pH rather than the mildly acidic pH 6.2 typical of vacuoles in wild-type strains (Preston *et al.*, 1989, 1992).

A closer examination of electron micrographs of the *pep7*Δ strain revealed the presence of multiple small vesicles distributed throughout the cytoplasm (Figure 5, A and C, low magnification, B and D, high magnification). The vesicles are indicated by arrows (Figure 5, B and D). These vesicles measure 40–60 nm in diameter. They are present at a frequency of 5.8 vesicles per mutant cell profile (n = 50, SD = 3.5) as compared with a frequency of 1.8 vesicles per wild-type cell profile (n = 50, SD = 1.2). Because plasma membrane-directed secretory vesicles have been demonstrated to measure approximately 100 nm in diameter (Novick *et al.*, 1981), the 40–60-nm vesicles seen to accumulate in *pep7* mutants are not likely to involve transport between the TGN and plasma membrane. However, it has been shown that intraorganelle transport vesicles found in the secretory and vacuolar pathways measure 30–60 nm (Novick *et al.*, 1981; Newman and Ferro-Novick, 1987; Shim *et al.*, 1991; Cowles *et al.*, 1994; Piper *et al.*, 1994; Becherer *et al.*, 1996), and therefore it is possible that the vesicles seen to accumulate in the *pep7* mutant may be a transport vesicle population. Because *pep7* mutants are not blocked in production of the secreted enzyme invertase (Garlow, 1989), it is unlikely that these accumulated vesicles result from a block in the secretory pathway.

The above data on vacuole morphology suggested that the lack of CPY activity seen in this mutant (the basis for isolation) was indeed due to perturbations in vacuolar function. Because CPY and other hydrolases are thought to be delivered from the TGN to the vacuole via vesicle-mediated transport ultimately (Vida *et al.*, 1993; Cowles *et al.*, 1994; Piper *et al.*, 1994; Becherer *et al.*, 1996), the accumulation of a 40–60-nm vesicle population in the *pep7* mutant suggested that this perturbation might be in transport of hydrolases in the vacuolar branch of the secretory pathway.

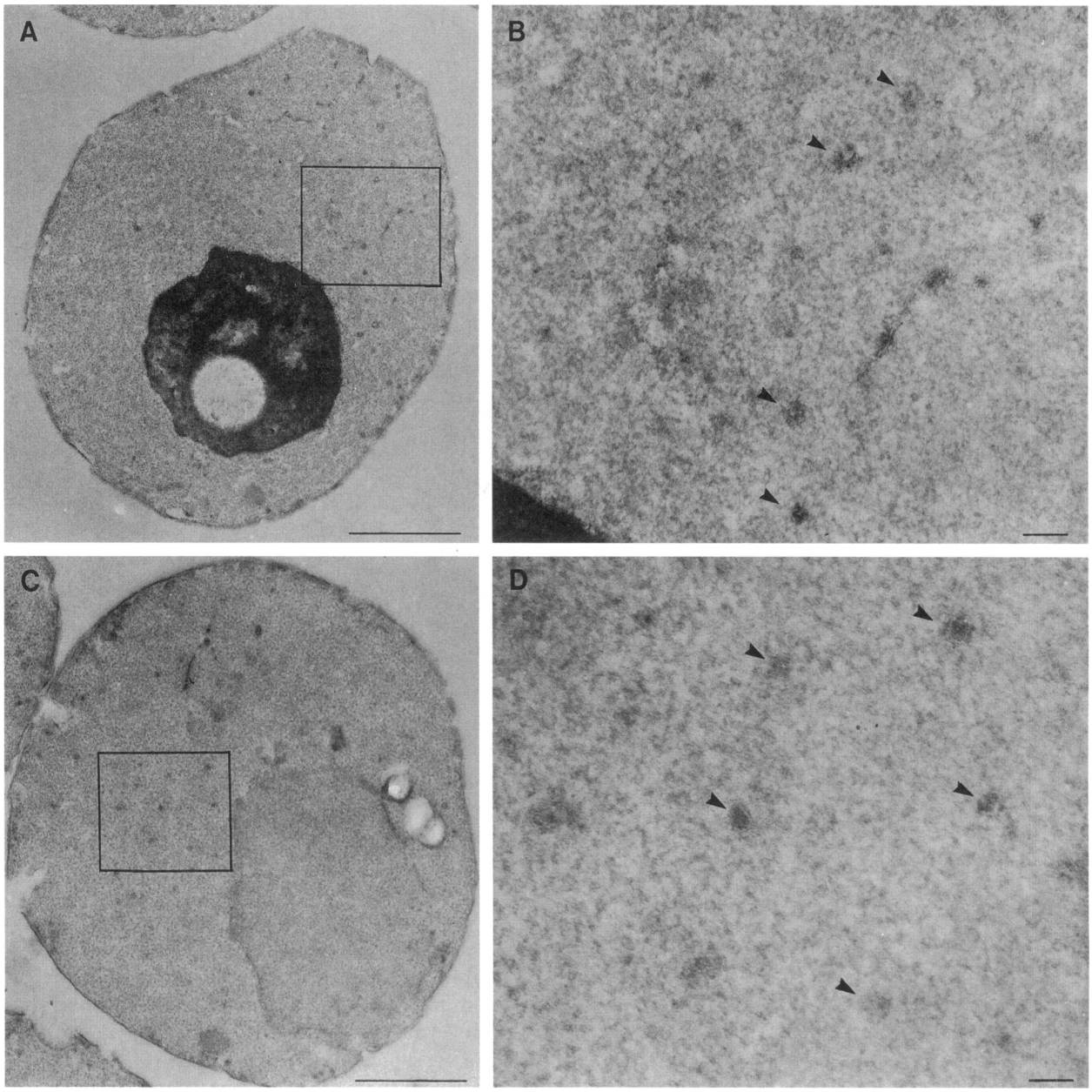

Figure 5. Vesicle accumulation in the *pep7*Δ mutant strain. Strain BJ8081 (*pep7*Δ::*LEU2*) was prepared and stained for electron microscopy as described in MATERIALS AND METHODS. (A and C) Low magnification views. Bars, 1 μm. Insets are shown at higher magnification in B and D, respectively. Bars, 100 nm. Arrows indicate vesicles seen in *pep7*Δ cells.

pep7 Mutants Demonstrate Sensitivity to Divalent Ions in Growth Medium

In wild-type cells, the vacuole is thought to be the site of divalent cation homeostatic regulation (Serrano, 1991). To test whether the vacuoles in *pep7* mutants are able to perform this function, both wild-type and *pep7*Δ strains were tested for the ability to grow on media containing excess divalent cations. Both wild-type and *pep7*Δ strains were streaked for single colonies on YEPD media containing either 3 mM $ZnCl_2$, 200 mM $CaCl_2$, 200 mM $SrCl_2$, or 3 mM $MnCl_2$. As noted in Figure 1 and Table 3, wild-type strains were able to grow robustly to form single colonies, whereas a *pep7*Δ strain showed very poor or no growth on $ZnCl_2$, $CaCl_2$, or $SrCl_2$ containing media and was slowed for growth on plates containing $MnCl_2$. This growth phenotype was not due to the excess Cl^- anion present, as 900 mM NaCl did not significantly

Table 1. Strain list

Saccharomyces cerevisiae	
BJ863	*MAT***a** *his5 s126*
BJ1983	*MATα trp1*
BJ2194	*MATα trp1 pep7-12*
BJ2202	*MATα trp1 pep7-13*
BJ2212	*MATα trp1 pep7-14*
BJ2218	*MATα trp1 pep7-15*
BJ2231	*MATα trp1 pep7-16*
BJ2329	*MATα trp1 pep7-10*
BJ2330	*MATα trp1 pep7-11*
BJ2406	*MAT***a** *ura3-52 leu2 trp1 pep7-11*
BJ2665	*MAT***a** *ura3-52 leu2*
BJ4000	*MATα ura3 leu2 trp1 his1 ade6 pep7Δ::LEU2*
BJ5124	*MAT***a** *ura3 leu2 pep7-17*
BJ5416	*MATα ura3-52 leu2Δ1 his3Δ200 lys2-801*
BJ7995	*MATα ura3 leu2 trp1 ade6 PEP7::HA*
BJ8081	*MAT***a** *ura3-52 leu2 pep7Δ::LEU2*
BJ8253	*MAT***a** *ura3-52 leu2 pep7-20*
BJ8286	*MATα ura3-52 leu2Δ1 his3Δ200 lys2-810 end4Δ::HIS3*
BJ8669	*MAT***a** *ura3-52 leu2 lys2-801 pep7-20 end4Δ::HIS3*
BJ8670	*MAT***a** *ura3-52 leu2 his3Δ200 pep7-20 end4Δ::HIS3*
BJ8751	*MAT***a** *ura3-52 leu2 lys2 bar1Δ::LYS2*
BJ8752	*MAT***a** *ura3-52 leu2 lys2 bar1Δ::LYS2 pep7-20*
BJ8753	*MAT***a** *ura3-52 leu2 lys2 bar1Δ::LYS2 pep7Δ::LEU2*
BJ8864	*MATα ura3-52 leu2Δ1 his3Δ200 lys2-801 pep7Δ::LEU2*
BJ8865	*MATα ura3-52 leu2Δ1 his3Δ200 lys2-801 end4Δ::HIS3*

impede growth. Furthermore, the growth defect is not likely to be a response to increased osmolarity, since inclusion of 1 M sorbitol did not impede growth. Included as a negative control, a strain deleted for the V-type ATPase subunit encoding gene *VAT2* was also severely inhibited for growth on media containing excess divalent ions. *vat2* mutants are unable to acidify their vacuoles and, therefore, thought to be unable to sequester divalent cations in the vacuole via vacuolar H^+/divalent cation antiporters (Serrano, 1991). These results with the *pep7* mutant suggest that the large vacuole found in *pep7* mutants is unable to buffer the cells against excess ions in the medium. Because *pep7* mutants have been demonstrated to be unable to acidify their vacuole (Preston *et al.*, 1992), it is possible that the ion^s phenotype is based on this pH defect.

pep7 Mutants Are Unable to Properly Process Vacuolar Hydrolases

pep7 mutants were analyzed for the ability to properly process and target the CPY precursor by metabolically radiolabeling spheroplasts and immunoprecipitating CPY from spheroplast fractions as well as from the medium in which the spheroplasts were incubated. In radiolabeling experiments, after a 20-min pulse and 30-min chase, a wild-type strain presented nearly all of the CPY antigen intracellularly as the mature enzyme (61 kDa), indicating proper delivery to the vacuole where the final processing reactions take place (Figure 6, lanes 1 and 2). The *pep7*Δ strain demonstrated a very different CPY antigen profile. The *pep7*Δ mutant strain secreted >89% of the CPY antigen into the medium as P2CPY (69 kDa; Figure 6, lanes 3 and 4), consistent with proper passage through the ER and Golgi, but lacking the final processing step(s) that indicates arrival at the vacuole (Figure 6, lane 4). Furthermore, the small fraction of CPY retained in the spheroplast fraction (<11%) is present as the P2 form, consistent with a block in transport somewhere between the Golgi compartment and the vacuole (Figure 6, lane 3).

To determine whether the lack of processing was specific to CPY, a similar analysis was carried out on three other vacuolar hydrolase: PrA, PrB, and ALP. The wild-type strain was able to process all three of these hydrolase precursors to mature forms during the 20-min pulse and 30-min chase (Figure 6, lanes 1 and 2), whereas all three of the hydrolase precursors failed

Table 2. Plasmid list

Plasmid	Insert	Vector
pBJ3952	10.5-kb genomic library complementing clone	YCp50
pBJ3953	3.8-kb *Sal*I *PEP7* fragment	YCp50 (*Sal*I)
pBJ3954	3.8-kb *Sal*I *PEP7* fragment	YIp5 (*Sal*I)
pBJ3958	*Bgl*II deletion of pBJ3954, *LEU2* *Bgl*II fragment inserted	YIp5 (*Sal*I)
pBJ3960	1.3-kb *Eco*RI/*Sal*I *PEP7* fragment	pATH11 (*Eco*RI/*Sal*I)
pBJ4272	3.8-kb *Sal*I *PEP7* fragment	YEp24
pBJ4639	1.8-kb *Eco*RV/*Hin*cII *PEP7* fragment	pTZ19R (*Sma*I)
pBJ4640	1.8-kb *Eco*RV/*Hin*cII *PEP7* fragment	pTZ18U (*Sma*I)
pBJ4928	1.8-kb *Eco*RV/*Sal*I *PEP7* fragment	YCp50
pBJ6171	1.8-kb *Eco*RV/*Hin*cII *PEP7* fragment	pKB711
pBJ7686	3.9-kb *Sal*I *PEP7::HA* fragment	YEp24
pBJ7687	2.0-kb *Sca*I/*Sal*I *PEP7* (*Not*I) fragment	pKB711 (*Eco*47III/*Sal*I)
pBJ7720	2.1-kb *Sca*I/*Sal*I *PEP7::HA* fragment	pKB711 (*Eco*47III/*Sal*I)
pBJ8168	2.0-kb *Sca*I/*Sal*I *pep7-20* fragment (original isolate)	pRS316 (*Sma*I/*Sal*I)
pBJ8234	2.0-kb *Sca*I/*Sal*I *pep7-20* fragment (subcloned)	pRS316 (*Sma*I/*Sal*I)

Table 3. Growth phenotype on media containing excess divalent ions

	YEPD containing						
	$ZnCl_2$	$CaCl_2$	$SrCl_2$	$MnCl_2$	NaCl	Sorbitol	------
PEP7	++	++	++	++	++	++	++
pep7Δ::LEU2	−	−	−	+/−	++	++	++
vat2Δ::LEU2	−	−	−	−	++	++	++

YEPD media containing the above listed divalent ions were made as described in MATERIALS AND METHODS. The final concentrations were 3 mM $ZnCl_2$, 200 mM $CaCl_2$, 200 mM $SrCl_2$, 3 mM $MnCl_2$, 900 mM NaCl, or 1 M sorbitol. Strains BJ2665 (*PEP7*), BJ8081 (*pep7Δ::LEU2*), and BJ6704 (*vat2::LEU2*) were streaked for single colonies on the above media and incubated for 2 d at 30°C. The resulting growth was scored as follows: ++, robust growth to single colonies; +, strong growth to single colonies; +/−, weak growth to single colonies; −, no growth to single colonies.

to undergo significant vacuolar processing in the *pep7Δ* strain (Figure 6, lanes 3 and 4). Like CPY, PrA and PrB were found in precursor forms consistent with transport through the ER and Golgi complex. Unlike CPY, however, which was secreted from the *pep7Δ* strain, the precursors to the soluble hydrolases PrA and PrB were not secreted into the medium in significant amounts. Because precursors to CPY, PrA, and PrB are thought to transit the same compartments en route to the vacuole (Klionsky *et al.*, 1990), this may be an indication that the sorting mechanism of CPY is significantly different from that utilized by PrA and PrB. The integral membrane hydrolase ALP, which was matured to its 72-kDa form in the wild-type strain (Figure 6, lane 1), was not processed in the *pep7Δ* strain but instead was found in a 76-kDa precursor form (Figure 6, lane 3), again consistent with transport through the ER and Golgi complex. Because ALP is an integral membrane protein, not surprisingly, nearly all of the precursor remained cell associated (Figure 6, lane 3).

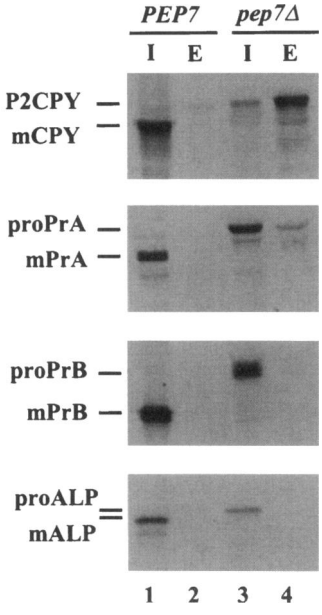

Figure 6. Sorting and processing of vacuolar hydrolases. Spheroplasts of strains BJ1983 (PEP7) and BJ4000 (*pep7Δ::LEU2*) were pulse-labeled with Tran^{35}S for 20 min and chased for 30 min at 30°C. The labeled cultures were separated into spheroplast (internal, I) and medium (external, E) fractions. Vacuolar hydrolases CPY, PrA, PrB, and ALP were immunoprecipitated from each fraction. The precipitated proteins were subjected to denaturing PAGE on gels of the following acrylamide concentrations: 8% for ALP, 10% for CPY and PrA, and 12% for PrB. Autoradiography was carried out as described in MATERIALS AND METHODS. The position of Golgi-modified precursor forms (P2CPY, proPrA, proPrB, and proALP) and mature vacuolar forms (mCPY, mPrA, mPrB, and mALP) of the hydrolases are indicated.

Isolation and Characterization of a pep7^{ts} Allele

Because the precursors to CPY, PrB, and ALP undergo PrA-dependent processing during their maturation (reviewed in Jones *et al.*, 1989; Klionsky *et al.*, 1990; Jones, 1991b; Jones and Murdock, 1994; Van Den Hazel *et al.*, 1996), it was possible that the effects of a loss of *PEP7* function on maturation of these hydrolases was a secondary effect due to loss of mature active PrA in *pep7Δ* strains. To address this concern of primary versus secondary effects of loss of *PEP7* function, a temperature-conditional allele of *PEP7* was generated by in vitro mutagenesis of plasmid-borne *PEP7* followed by transformation into a *pep7Δ* strain. Transformants were screened for temperature conditional growth on YEPD medium containing 6 mM $ZnCl_2$. A single colony was found whose contained plasmid caused a conditional Zn^s phenotype after shuttling the plasmid through *E. coli* (Figure 7A). This *PEP7* allele was designated *pep7–20*. A single nucleotide change was found in *pep7–20* DNA that changes Cys 252 to Trp (Figure 2). The *pep7–20* mutant proved to be conditionally defective for CPY targeting and maturation. At both the permissive (23°C) and restrictive temperatures (37°C), wild-type cells were able to process nearly all CPY to the mature 61-kDa size (Figure 7B, lanes 1 and 4), whereas a strain deleted for *PEP7* was unable to process P2CPY at either temperature (Figure 7B, lanes 3 and 6). At the permissive temperature a strain carrying the *pep7–20* allele was able to process CPY nearly as well as the wild-type strain (lane 2), but was as defective as the deletion strain at the restrictive temperature (lane 5). Therefore, the *pep7–20* mutant showed nearly wild-type function at the permissive temperature, but was nearly completely nonfunctional at the restrictive temperature.

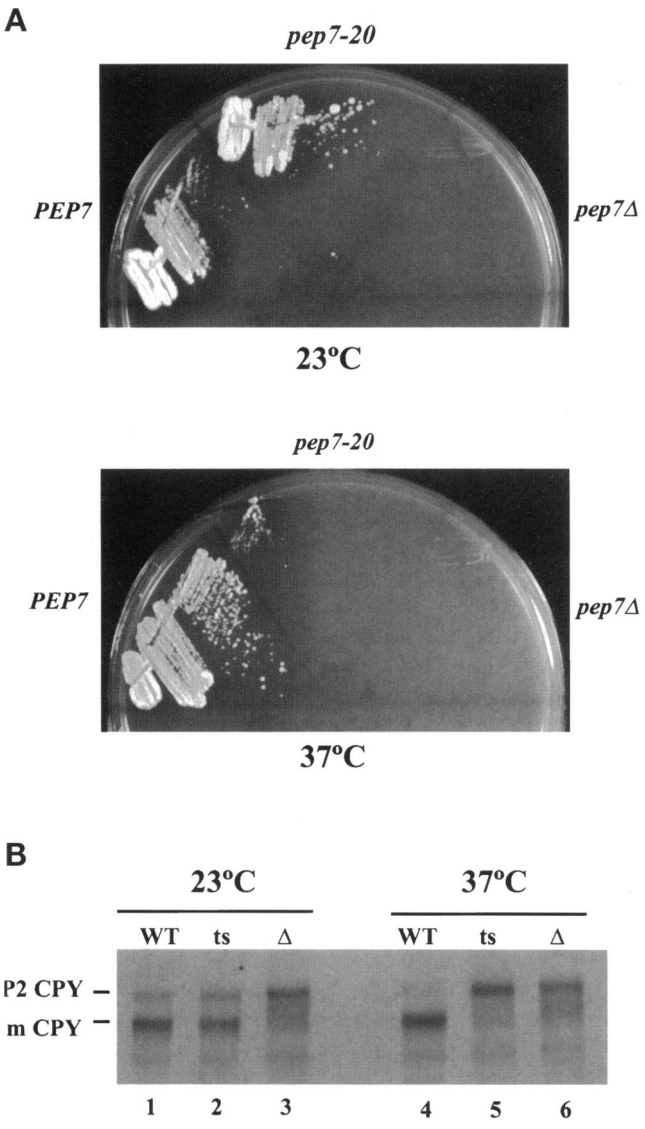

Figure 7. Isolation of a *pep7* temperature-conditional allele. (A) The *pep7–20* mutation was generated by in vitro mutagenesis of plasmid-borne *PEP7* DNA. The resulting DNA was transformed into strain BJ8081 (*pep7Δ::LEU2*) yielding transformants that were screened for temperature-conditional growth on YEPD containing 6 mM $ZnCl_2$. One plasmid conferred the desired temperature-sensitive growth phenotype. This allele was designated *pep7–20*. Shown are strains BJ2665 (*PEP7*), BJ8081 transformed with centromeric plasmid-based *pep7–20* DNA, pBJ8234 (*pep7–20*), and BJ8081 (*pep7Δ*) grown on 6 mM $ZnCl_2$ YEPD at both 23 and 37°C. (B) The same strains described in A were grown at 23°C to early log phase (*PEP7* = WT, *pep7–20* = ts, and *pep7Δ* = Δ). Cells were preincubated for 10 min at either 23°C or 37°C prior to labeling at the respective temperatures. The cells were pulse-labeled for 5 min with Tran^{35}S and chased for 45 min. Extracts were made by glass bead breaking. CPY was immunoprecipitated, separated on a 10% polyacrylamide gel, and subjected to autoradiography as described in MATERIALS AND METHODS. The position of the Golgi-modified precursor CPY (P2CPY) and mature vacuolar CPY (mCPY) are indicated. (C) Spheroplasts of strain BJ8081 carrying plasmid pBJ8234 (*pep7–20*) were preincubated at 37°C for 5 min. A pulse-label with Tran^{35}S was initiated and carried out at 37°C. At 1, 2.5, 5, 10, and 15 min after pulse, one-fifth of the culture was removed and a 25-min chase was carried out on the aliquot at 37°C. The labeled aliquots were treated as described in Figure 6. CPY was immunoprecipitated from the fractions, separated on a 10% polyacrylamide gel, and subjected to autoradiography as described in MATERIALS AND METHODS.

To assess the kinetics of induction of the mutant phenotype in a *pep7–20* strain, spheroplasts of a single large *pep7–20* culture were preincubated at 37°C for 5 min followed by the addition of label. At 1, 2.5, 5, 10, or 15 min after labeling one-fifth of the culture was removed and subjected to a 25-min chase with nonradioactive cysteine and methionine at 37°C. CPY was immunoprecipitated from both cell (internal) and medium (external) fractions. This experimental regimen allows a determination of the time of onset of the secretion and processing defects. At the first time point examined (5-min temperature shift, 1-min labeling, 25-min chase), the mutant cells were unable to transport a significant fraction of CPY to the vacuole as determined by the lack of internal mature CPY (Figure 7C, lane 1). As cells at this time point, like all those following, underwent a 25-min chase incubation, the block in transport to the vacuole appears to be firmly in place. Additionally, the mutant secreted a significant fraction of the P2CPY into the medium (Figure 7C, lane 2). This same trend is continued at later time points (Figure 7C, lanes 3–10). These data indicate that the Pep7p function must have been inactivated during the 5-min preincubation and that the sorting and processing defects were manifested very rapidly upon loss of Pep7p function. The data thus imply that a primary function of Pep7p is in transport and/or sorting of CPY at a step distal to Golgi modification.

pep7^{ts} Mutants at Restrictive Temperatures Are Blocked in Transport of Three Soluble Vacuolar Hydrolases, But Not a Membrane Vacuolar Hydrolase

To address the extent of pleiotropy attendant on loss of *PEP7* function, the production of CPY, PrA, PrB, and ALP in radiolabeled spheroplasts was examined

at both 23°C and 37°C. Wild-type, *pep7–20*, and *pep7Δ* strains were grown at 23°C to early log phase, spheroplasts were formed, the cultures were split, and one-half was incubated for 5 min at 37°C while the other half continued to incubate at 23°C. The spheroplasts were then radiolabeled in a pulse-chase experiment. CPY, PrA, PrB, and ALP were immunoprecipitated from both spheroplast extracts (internal) and medium fractions (external). The wild-type strain was able to process the great majority of all four hydrolases at either temperature (Figure 8, lanes 1 and 2). The *pep7Δ* strain was unable to efficiently process any of the hydrolase precursors at either temperature, and again secreted a significant fraction of CPY into the medium (Figure 8, lanes 5 and 6). For synthesis, transport, and processing of the CPY, PrA and PrB precursors, at 23°C the *pep7–20* mutant looked strikingly like the wild-type strain, but at 37°C the conditional mutant looked like the *pep7Δ* strain (Figure 8, A–C, lanes 3 and 4). This includes the slightly aberrant secretion of CPY demonstrated by both the wild-type and *pep7–20* strains at 23°C (Figure 8A, lanes 2 and 4). These data indicate that the lack of processing of hydrolase precursors of CPY, PrA, and PrB is due to a nearly immediate block of transport at some step between the Golgi and the vacuole upon loss of *PEP7* function and not secondarily due to depletion of vacuolar pools of mature processing proteases in the vacuoles of *pep7* strains.

The synthesis of ALP, however, presented a different profile. Like the wild-type strain, the *pep7–20* mutant was able to efficiently synthesize and process the ALP precursor at both the permissive and restrictive temperatures (Figure 8D, lanes 1–4), therefore suggesting that the vacuole in the conditional mutant at the restrictive temperature was not only competent to receive vesicle traffic from the secretory path, but that it was also still competent to carry out PrA-dependent processing of the ALP precursor. Because all of the newly synthesized PrA precursor was precluded from reaching the vacuole, as demonstrated by its failure to be processed to mature form at 37°C (Figure 8B, lanes 3 and 4), processing of the ALP precursor must be catalyzed by the PrA delivered to the vacuole and proteolytically processed prior to the temperature shift and radiolabeling. The fact that the ALP precursor was processed to its mature form at the restrictive temperature indicates that this hydrolase precursor can reach the vacuole via a Pep7p-independent mechanism.

ALP Does Not Reach the Vacuole via Endocytosis in pep7^{ts} Mutants at Restrictive Temperatures

Because ALP was able to reach the vacuole via a Pep7p independent mechanism (Figure 8D, lane 3), we determined whether ALP travels to the vacuole via endocytosis (Nothwehr *et al.*, 1995). Strains were constructed that carried both the *end4Δ* mutation and the temperature-sensitive allele *pep7–20*, and therefore precluded delivery to the vacuole via endocytosis (Raths *et al.*, 1993). In pulse-chase experiments, a wild-type strain was able to process ALP to the mature size (76 kDa) as expected (Figure 9A, lane 1). Furthermore, an *end4Δ* strain was also able to process ALP (Figure 9A, lanes 4 and 8), as ALP does not usually travel to the vacuole via the plasma membrane (Nothwehr *et al.*, 1995). Again, a *pep7Δ* strain was unable to process precursor ALP to its mature form (Figure 9A, lane 2), whereas a *pep7–20* mutant was able to process precursor ALP to its mature size at both permissive and restrictive temperatures (Figure 9A, lanes 3 and 7). Two different *pep7–20 end4Δ* doubly mutant strains were able to process the ALP precursor at both permissive (Figure 9A, lanes 5 and 6) and restrictive temperatures (Figure 9A, lanes 9 and 10), demonstrating that in the absence of Pep7p function, the precursor to ALP was routed to the vacuole, but this route was not via the plasma membrane.

To ensure that a thermal block of *PEP7* function had been induced under the conditions of the experiment in Figure 9A, CPY was immunoprecipitated from the same extracts (Figure 9B). As expected, neither wild-type nor *end4Δ* strains showed a defect in CPY processing (Figure 9B, lanes 1, 4, and 8), whereas a *pep7Δ* stain showed little or no processing (Figure 9B, lane 2). The strains containing *pep7–20* either alone or with *end4Δ* were fully capable of processing the CPY precursor at the permissive temperature as expected (Figure 9B, lanes 3, 5, and 6), but were severely defective in precursor CPY processing at the restrictive temperature (Figure 9B, lanes 7, 9, and 10), indicating that the thermal block had been successfully induced.

Interestingly, whereas the strain carrying the *pep7–20* allele alone had the predicted CPY phenotypes at the restrictive temperature (complete lack of P2CPY processing; Figure 9B, lane 7), the *pep7–20 end4Δ* double mutants both processed some small amount of P2CPY to a mature form at the restrictive temperature (Figure 9B, lanes 9 and 10). The significance of this observation is not immediately evident, except to suggest that perturbations to the endocytic pathway impinge on the Golgi to vacuole traffic. Alternatively, because these strains are not isogenic, this small variation in phenotype may originate from variation in the genetic background of these three strains.

Endocytosis in pep7 Mutants

Studies in class E vacuolar protein-sorting mutants have led to the hypothesis that transport between the TGN and vacuole merge with transport between the plasma membrane and the vacuole at a common endosomal compartment (Davis *et al.*, 1993; Piper *et al.*,

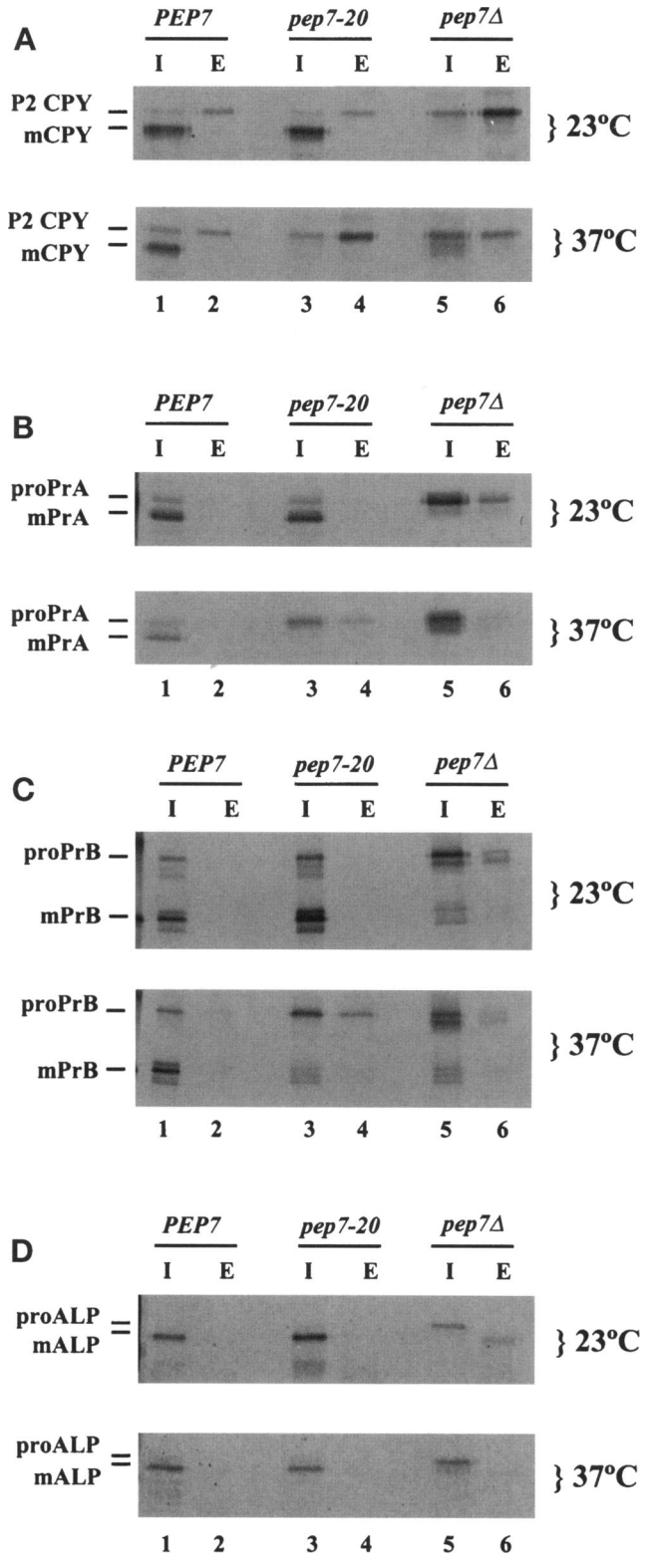

Figure 8. Vacuolar hydrolase sorting and processing in the *pep7–20* mutant. Spheroplasts of strain BJ8081 carrying the plasmid pBJ8271 (*PEP7*), the plasmid pBJ8234 (*pep7–20*), or pRS316 (*pep7Δ*) were preincubated at the indicated temperatures for 5 min. The spheroplasts were pulse-labeled with Tran^{35}S at the indicated temperatures for 5 min and chased for 45 min. Labeled cultures were treated as described in Figure 6. The positions of Golgi-modified precursor forms (P2CPY, proPrA, proPrB, and proALP) and mature vacuolar forms (mCPY, mPrA, mPrB, and mALP) of the hydrolases are indicated.

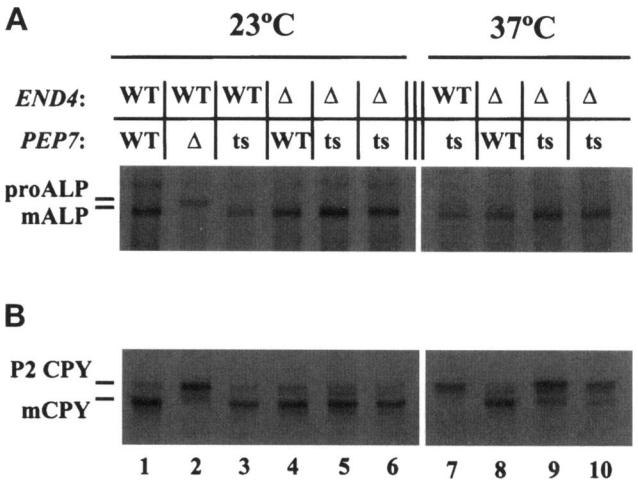

Figure 9. ALP processing in *pep7–20/end4Δ* strains. Strains BJ2665 (WT), BJ8081 (*pep7Δ*), BJ8253 (*pep7ts*), BJ8286 (*end4Δ*), BJ8669 (*pep7ts, end4Δ*), and BJ8670 (*pep7ts, end4Δ*) were preincubated for 5 min at either 23°C or 37°C as indicated. A 5-min pulse-label with Tran^{35}S followed by a 45-min chase at the respective temperatures was carried out. Cell extracts were made by glass bead breaking. ALP (A) and CPY (B) were immunoprecipitated from the labeled extracts and separated on 8 and 10% polyacrylamide gels, respectively. Autoradiography was carried out as described in MATERIALS AND METHODS. The positions of both Golgi-modified precursor forms of the hydrolases (proALP and P2CPY) and mature vacuolar forms (mALP and mCPY) are indicated.

1995; Rieder *et al.*, 1996). Therefore, we were interested in testing whether the loss of Pep7p function impinges upon endocytic processes. To test fluid phase endocytosis, the ability of a *pep7* mutant strain to take up and deliver Lucifer yellow to the vacuole was tested. A wild-type strain endocytosed and accumulated Lucifer yellow in the vacuole (Figure 10A). The vacuole is identified by its prominent profile in the Nomarski exposure (Figure 10, B, D, and F). The *pep7Δ* strain appeared to take up Lucifer yellow nearly as well as the wild-type strain did (Figure 10C). As expected, an *end4* mutant, which is unable to carry out endocytosis (Raths *et al.*, 1993), does not take up Lucifer yellow (Figure 10C).

Furthermore, we investigated the ability of *pep7* mutants to carry out receptor-mediated endocytosis. We first assayed *pep7* mutants for internalization of α-factor at both 23°C and 37°C. An isogenic wild-type strain was tested and demonstrated no defect for in-

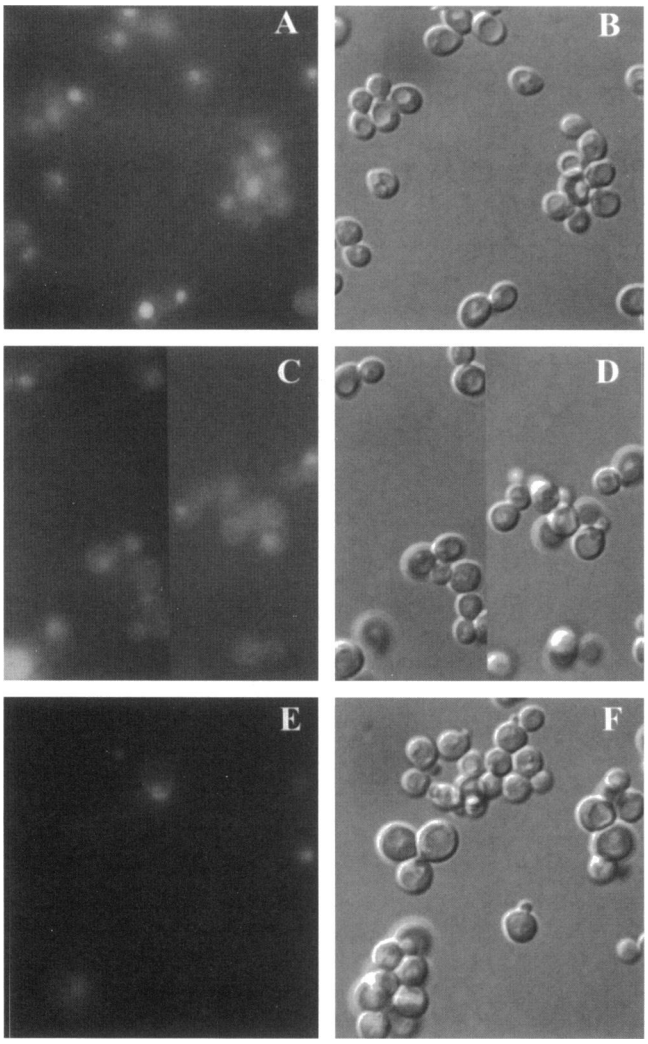

Figure 10. Lucifer yellow uptake by *pep7* mutants. Isogenic strains BJ5416 (*PEP7*), BJ8864 (*pep7Δ::LEU2*), and BJ8865 (*end4Δ::HIS3*) were tested for their ability to take up and deliver fluid-phase endocytotic marker Lucifer yellow to the vacuole as described in MATERIALS AND METHODS. Fluorescence and Nomarski images of the same field of cells were acquired using a multimedia fluorescence microscope fitted with FITC and Nomarski optics. Shown are fluorescence and Nomarski images, respectively, of BJ5416 (*PEP7*; A and B), BJ8864 (*pep7Δ::LEU2*; C and D), and BJ8865 (*end4Δ::HIS3*; E and F).

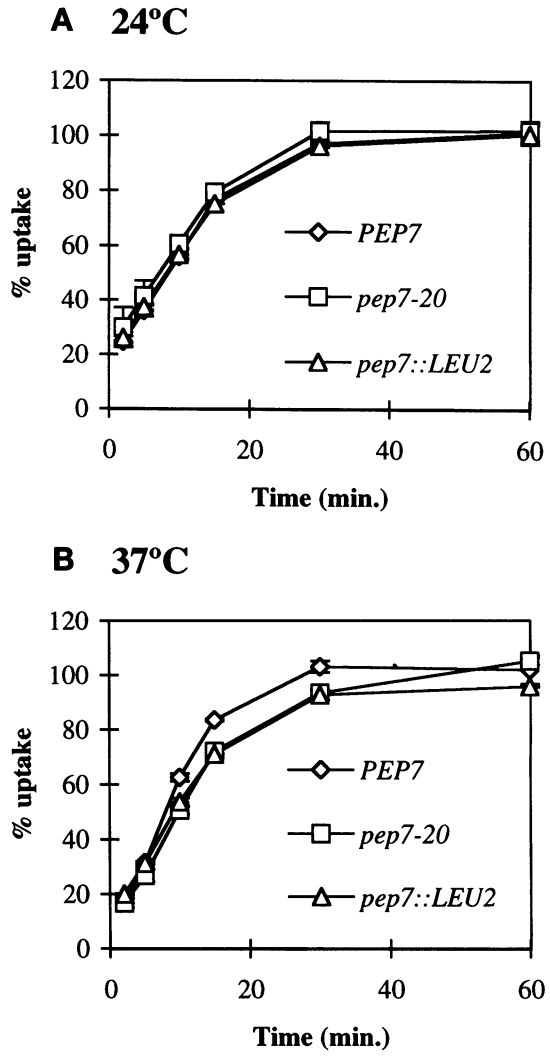

Figure 11. α-factor uptake from the plasma membrane in *pep7* mutants. Isogenic strains BJ8751 (*PEP7*), BJ8752 (*pep7–20*), and BJ8753 (*pep7Δ::LEU2*) were tested for their ability to take up radiolabeled α-factor via receptor-mediated endocytosis as described in MATERIALS AND METHODS. Cells were preincubated for 10 min at either 24°C (A) or 37°C (B) prior to carrying out the uptake assay at these respective temperatures. The percentage of uptake was determined by a scintillation counter. The amount of pheromone internalized was divided by the total cell-associated pheromone and this was multiplied by 100 to equate percentage of uptake. The assay was performed twice and SDs are shown by error bars.

ternalization capabilities at either 23 or 37°C (Figure 11, A and B). Uptake of α-factor in both *pep7Δ* and *pep7–20* mutants at both the permissive and restrictive temperatures demonstrated nearly wild-type kinetics (Figure 11, A and B). Then we tested the *pep7–20* conditional mutant for the ability to deliver the endocytosed α-factor to the vacuole by assaying for vacuolar degradation of endocytosed pheromone. The wild-type strain internalized nearly all of the surface bound α-factor within 7.5 min at 24°C. Compare Figure 12A, lane 1 (total bound pheromone) to lanes 2 (0-min internalization) and 3 (7.5-min internalization). Degradation of the intact α-factor was evident by 30 min (Figure 12A, lane 5) and was nearly complete at the 60-min time point (Figure 12A, lane 6). This wild-type strain behaved similarly at 37°C (Figure 12B, B). The isogenic *pep7–20* mutant was nearly indistinguishable from the wild-type strain at 24°C for both uptake and degradation (Figure 12C). At 37°C, this conditional mutant showed wild-type uptake kinetics (Figure 12D, lanes 1–3); however, the mutant was signifi-

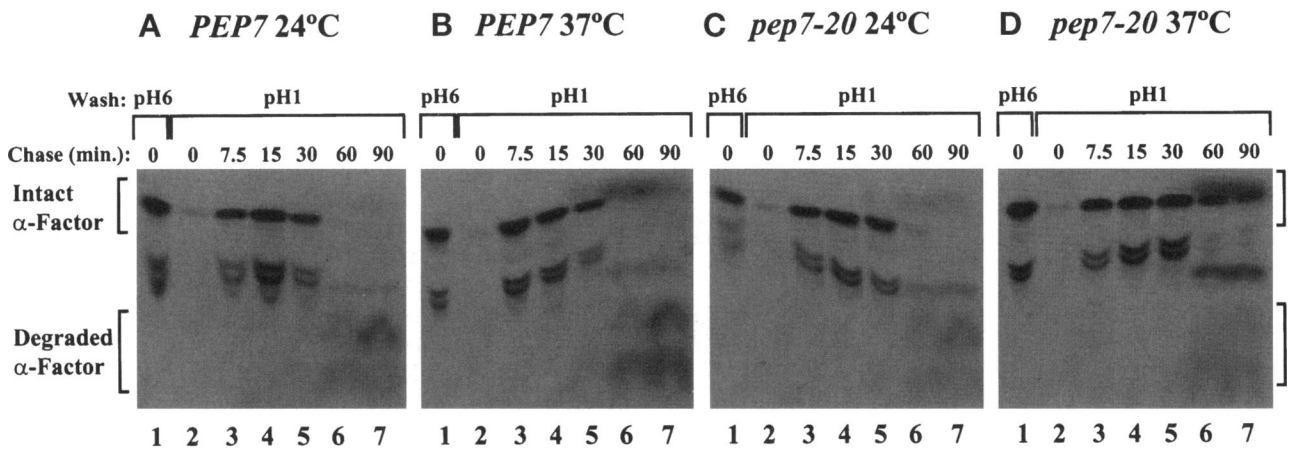

Figure 12. Delivery of radiolabeled α-factor to the vacuole in *pep7* mutants. Isogenic strains BJ8751 (*PEP7*; A and B) and BJ8752 (*pep7–20*; C and D) cultured at 24°C were allowed to bind ^{35}S-labeled α-factor for 1 h on ice followed by incubation at either 24°C (A and C) or 37°C (B and D). At the indicated time after the temperature shift, aliquots were taken and diluted into pH 6 or pH 1 buffer to measure internalization. α-factor degradation was assayed by extracting cell-associated radiolabel, separating the components on TLC plates, and carrying out autoradiography as described in MATERIALS AND METHODS. Intact and degraded α-factor are indicated.

cantly blocked in transport of the internalized α-factor to the vacuole as indicated by the persistence of intact pheromone 90 min into the assay (Figure 12D, lane 7).

Pep7p Is Found as Both a Soluble Cytoplasmic Protein and Associated with a Particulate Cellular Compartment

We have utilized two approaches to localize Pep7p. In the first, we determined whether Pep7p was enriched in particular organelle preparations. Because the *pep7* mutant phenotype involves vacuole function but the protein structure (zinc finger domains and putative nuclear localization sequences) might suggest a nuclear involvement, standard procedures were used to purify nuclei (Kalinich and Douglas, 1989) and vacuoles (Woolford *et al.*, 1990). The latter fraction almost certainly enriches for endosomal compartments, and therefore is considered a preparation of vacuolar pathway components (at least vacuole and endosomes; Becherer and Jones, personal communication). In immunoblots of the purified organelle fractions, the 95-kDa integral membrane subunit of the vacuolar ATPase (Vph1p) was highly enriched in the vacuolar/endosomal preparation (Figure 13, lanes 3 and 4) and was not enriched in unfractionated cell extracts or nuclear preps (Figure 13, lanes 1, 2, and 5). This is consistent with its localization in the vacuolar membrane. This ATPase subunit was also retained in a membrane fraction derived from the vacuole/endosomal preparation, as expected for an integral membrane protein (Figure 13, lane 4). Antibodies to RNA polymerase II were used to determine the fractionation profile of soluble nuclear components. RNA polymerase II was found in the nuclear fraction (Figure 13, lane 2), but was significantly depleted in the vacuolar/endosomal fractions (Figure 13, lanes 3 and 4). Pep7p, blotted with polyclonal antibodies raised to a TrpE-Pep7p fusion protein (see MATERIALS AND METHODS), was highly enriched in endosomal/vacuolar fractions as well as in membrane preparations derived from this preparation (Figure 13, lanes 3 and 4). The observed enrichment of Pep7p in the vacuole/endosomal preparations was not due to TGN contamination, as TGN marker Kex2p did not show a similar enrichment (Figure 13, lanes 3 and 4). As expected, the lumenal vacuolar marker, PrA, showed a substantial

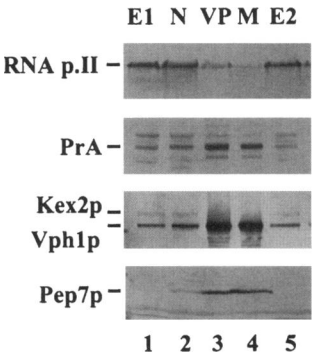

Figure 13. Localization of Pep7p by organelle preparation. Nuclei (N) were purified from a cell extract of strain BJ1983 (E1) as described in MATERIALS AND METHODS. Vacuolar pathway organelles (VP), and vacuolar pathway organelle membranes (M) were also purified from a second cell extract from strain BJ1983 (E2) as described in MATERIALS AND METHODS. Equal amounts of protein of each fraction were separated on denaturing polyacrylamide gels followed by immunoblotting with polyclonal antibodies to organelle marker proteins and Pep7p. RNA polymerase II (RNA p.II) was used as a nuclear marker. PrA and Vph1p were used as vacuolar pathway markers. Kex2p was used as a TGN marker. RNA p.II and Pep7p were blotted from the same gel that received 75 μg of protein/lane. Kex2p and Vph1p were blotted from the same gel that received 5 μg of protein/lane. PrA was immunoblotted from a gel that received 5 μg of protein/lane. The positions of the marker proteins and Pep7p are indicated.

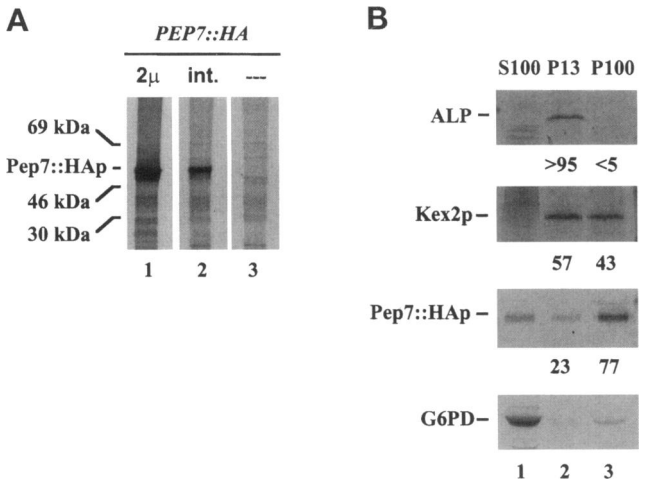

Figure 14. Subcellular fractionation of Pep7p. (A) Spheroplasts of strains BJ4000 transformed with pBJ7686 (*PEP7::HA*/2μ), BJ7995 (containing the *PEP7::HA* construct integrated at the *PEP7* locus) (*PEP7::HA*/int.), and BJ4000 (*PEP7::HA*/—) were pulse-labeled with $Na_2{}^{35}SO_4$ for 90 min at 30°C. The spheroplasts were lysed and Pep7::HAp was immunoprecipitated from the labeled cell extracts with monoclonal antibody that recognizes the HA epitope (12CA5). The precipitated protein was separated on a 10% polyacrylamide gel and subjected to autoradiography as described in MATERIALS AND METHODS. The position of the epitope-tagged Pep7p is indicated. (B) Spheroplasts of strain BJ7995 were pulse-labeled with Tran^{35}S for 30 min, and chased for 60. The spheroplasts were lysed and fractionated by differential centrifugation. First, the lysate was subjected to centrifugation at 13,000 × *g*, yielding a low-speed pellet (P13) and a low-speed supernatant fraction. The supernatant fraction was then subjected to a second centrifugation at 100,000 × *g*, resulting in a high-speed pellet (P100) and high-speed supernatant (S100). Pep7::HAp was immunoprecipitated from each of the indicated fractions, as were the following marker proteins: ALP (vacuole), Kex2p (TGN), and glucose 6-phosphate dehydrogenase (G6PD, cytoplasm). The precipitated proteins were separated on polyacrylamide gels (Pep7::HAp and G6PD on a 10% gel; ALP and Kex2p on 8.5% gel) and subjected to autoradiography as described in MATERIALS AND METHODS. Quantitation of the autoradiographs was carried out on an Ambis 4000 optical imager using core software version 4.0 and is indicated below the pellet fractions as the percentage of the total amount of the antigen that pelleted in either the P13 or P100 pellets.

enrichment in the vacuole/endosome preparation, like Vph1p and Pep7p (Figure 13, lane 3). However, unlike Pep7p and Vph1p, PrA was somewhat diminished in preparation of membranes from this fraction (Figure 13, lane 4). This agrees with the observation that Pep7p does not appear to contain a signal sequence and would not be expected to enter the secretory pathway and thus reside as a soluble lumenal protein.

In conjunction with these experiments, whole-cell fractionation via differential centrifugation was carried out on cell extracts from radiolabeled spheroplasts. The polyclonal antibodies used above for immunoblotting Pep7p were ineffective in precipitating Pep7p in single or high copy from radiolabeled cell extracts. Therefore, a triple HA epitope tag was introduced at the C terminus of Pep7p by cloning. *PEP7::HA* was able to fully complement the *pep7Δ::LEU2* mutation (Figure 1). Monoclonal antibodies that recognize this epitope tag precipitated a Pep7::HAp-specific protein in extract from cells carrying this construct, but not from cells lacking this construct (Figure 14A, lanes 2 and 3). Expression of this construct from a high copy vector led to its overexpression (Figure 14A, lane 1).

Radiolabeled cell extracts were subjected to differential centrifugation to separate the various organelles on the basis of velocity sedimentation as described in Becherer *et al.* (1996). Lysates were fractionated by centrifugation into a 13,000 × *g* pellet (P13), a 100,000 × *g* pellet (P100), and a 100,000 × *g* supernatant (S100). Nearly all of the vacuolar protein ALP was found in the P13 fraction (>95%; Figure 14B, lane 2), whereas the TGN protein Kex2p was approximately equally distributed between the P13 and P100 fractions (57% and 43%, respectively; Figure 14B, lanes 2 and 3). Pep7p fractionated neither like TGN nor vacuolar proteins. Instead it was found both as a soluble protein in the S100 fractions and as a pelletable protein (Figure 14B, lanes 1–3). Furthermore, the population of Pep7p that pelleted with the cellular membranes presented a distribution pattern distinct from those of both TGN and vacuolar proteins. Pep7p was enriched in the P100 fraction (>75%), suggesting that the pelletable fraction of Pep7p may be associated with an organelle smaller than either the TGN membranes or the vacuolar membranes. Because of the above described mutant phenotypes, this might be predicted to be either the endosome or a transport vesicle that mediates transport between the TGN, endosome, and/or vacuole.

To further study the association between Pep7p and cellular membranes and to determine whether Pep7p was wholly exposed to the cytoplasm as predicted, radiolabeled unfractionated cell extracts were subjected to a protease K protection assay followed by immunoprecipitation. Immunoprecipitates from extract treated with neither protease nor detergent contained stable Pep7p (Figure 15A, lane 1). Pep7p was fully digested by exogenously added protease K both in the absence and presence of detergent (Triton X-100) to dissolve cellular membranes (Figure 15A, lanes 2 and 3). This observation indicates that all of Pep7p, both that in the soluble pool (as expected) as well as the membrane-associated fraction, is exposed to the cytoplasm. As a control for membrane integrity, ALP was immunoprecipitated from the same extracts. ALP serves as a particularly good control for membrane integrity in protease K protection assays as an antigen of unique size is found for each of the three assay conditions (Klionsky and Emr, 1989). The mature 72-kDa ALP

(Figure 15A, lane 1) contains two domains that are susceptible to protease K digestion. The N-terminal cytoplasmic tail of approximately 30 amino acids can be proteolyzed in the absence of detergent (Figure 15A, lane 2), and a short C-terminal lumenal domain can be additionally removed if detergent is added with protease K, leaving a core domain that is resistant to further proteolysis (Figure 15A, lane 3). The fact that only ALP of the intermediate size was present in extracts that had been treated with protease K alone indicates that membrane compartments were sealed and, therefore, that Pep7p must lie outside cellular organelles.

To characterize the interaction of Pep7p and the cellular membrane(s), a similarly labeled whole-cell extract was treated with 1 M NaCl, 5 M urea, or as control, unaltered lysis buffer, followed by immunoprecipitation. Control treatment of extracts with lysis buffer again revealed Pep7p in both a soluble and pelletable fraction (Figure 15B, lanes 5 and 6). Extraction with 1 M NaCl solublizes Pep7p (Figure 15B, lanes 1 and 2), indicating that Pep7p associates with cellular organelles through ionic interactions. Finally, 5 M urea was able to solublize Pep7p (Figure 15B, lanes 3 and 4), further indicating that Pep7p is not held in a complex by covalent interactions. As a control for membrane integrity, integral membrane protein ALP was also immunoprecipitated from the samples. As expected, the distribution of ALP was not altered by treatment with lysis buffer (Figure 15B, lanes 5 and 6) or NaCl (Figure 15B, lanes 1 and 2). Five molar urea was able to partially extract ALP into the soluble fraction (Figure 15B, lanes 3 and 4), indicating that this extraction, though harsh, was not sufficient to completely dislodge integral membrane proteins. Because 5 M urea was sufficient to completely move Pep7p into the soluble fraction, this suggests that Pep7p, as expected, is not likely to be an integral membrane protein.

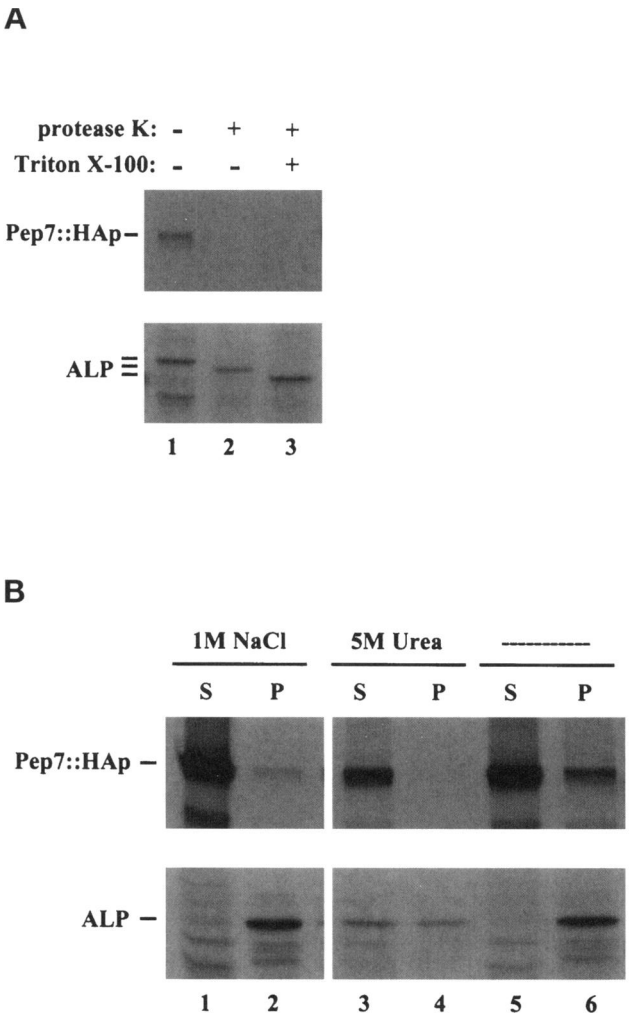

Figure 15. Protease K protection assay and extraction assay of Pep7::HAp. (A) Spheroplasts of strain BJ7995 were pulse-labeled with $Na_2{}^{35}SO_4$ for 60 min and chased for 20 min. The spheroplasts were lysed and treated with protease K and/or Triton X-100 as indicated. The reactions were stopped by the addition of TCA to 20%. Both Pep7::HAp and ALP were immunoprecipitated from the resulting protein extracts, separated on polyacrylamide gels (10% polyacrylamide for Pep7::HAp and 8.5% polyacrylamide for ALP), and subjected to autoradiography as described in MATERIALS AND METHODS. (B) Spheroplasts of strain BJ7995 were radiolabeled and an extract made as described in MATERIALS AND METHODS. The cell extract was divided into three equal aliquots and treated with equal volumes of one of the following: 2 M NaCl in lysis buffer (final concentration of 1 M NaCl), 10 M urea in lysis buffer (final concentration of 5 M urea), or unmodified lysis buffer (——). The samples were then centrifuged at 100,000 × *g* to produce a high-speed supernatant (S) and high-speed pellet (P). Both Pep7::HAp and ALP were immunoprecipitated from the resulting fractions, separated on polyacrylamide gels (10% polyacrylamide for Pep7::HAp and 8.5% polyacrylamide for ALP), and subjected to autoradiography as described in MATERIALS AND METHODS.

DISCUSSION

PEP7 is one of over 40 genes thought to function in some capacity in vacuolar hydrolase synthesis, and as such offers an opportunity to study how the synthesis and targeting of proteins are brought about in the partitioned eukaryotic cell.

Comparison of the Pep7p protein sequence in various databases revealed several sequence motifs held in common with a variety of proteins. The N-terminal two-thirds of Pep7p contains several cysteine-rich regions. The most N-terminal of these (AA 8–29) is similar in sequence to the zinc finger motif found in transcription factor TFIIIA from *X. laevis* (Berg, 1990; Figure 3A). Also, amino acids 212–294 show striking sequence similarity to tripartite cysteine-rich regions found in yeast genes *VPS27* and *FAB1*, both of which are thought to impinge upon vacuolar function (Piper *et al.*, 1995; Yamamoto *et al.*, 1995; Figure 3B). The similarity between these proteins has been noted pre-

viously (Piper *et al.*, 1995). Other uncharacterized yeast ORFs as well as proteins and ORFs from higher eukaryotes also contain this sequence motif (Figure 3B). This tripartite motif is essential for Pep7p function as demonstrated by the observation that all missense alleles uncovered in this study change conserved cysteine residues in this motif to tyrosine or tryptophan.

The N terminus of Pep7p also contains sequences with similarity to known nuclear localization sequences (Robbins *et al.*, 1991; Gorlich *et al.*, 1995; Figure 3C). Despite this sequence similarity, it does not appear that these stretches of amino acids function as a nuclear localization sequence in Pep7p. In the process of sequencing various *PEP7* mutant alleles, silent mutations were found that changed conserved amino acids in these motifs (Figure 2). Additionally, neither localization studies nor phenotypic analysis are consistent with a nuclear localization of Pep7p (see below).

The C-terminal one-third of Pep7p (amino acids 295–515) shows characteristics of a heptad repeat motif (Hodges *et al.*, 1972; Hu *et al.*, 1990) that often function in protein–protein interactions (Hu *et al.*, 1990). Nonsense mutations found in alleles *pep7–16* and *pep7–17* truncate part or nearly all of this region and lead to a null phenotype. Therefore, this region of the protein, whatever its structure, is necessary for Pep7p function.

pep7 mutants were isolated as CPY deficient (Jones, 1977). CPY, like several other vacuolar hydrolases, is known to be transported to the vacuole via the secretory pathway (reviewed in Klionsky *et al.*, 1990; Van Den Hazel *et al.*, 1996). In a TGN-like compartment these vacuolar hydrolases are sorted away from the secreted proteins (Graham and Emr, 1991). The vacuolar hydrolases are transported first to the endsome and subsequently to the vacuole (Vida *et al.*, 1993). These steps in the vacuolar pathway are thought to be accomplished via vesicle-mediated transport utilizing specific SNARE complex components (Cowles *et al.*, 1994; Piper *et al.*, 1994; Becherer *et al.*, 1996). The following observations presented in this study demonstrate that Pep7p acts directly on transport of hydrolases through the vacuolar branch of the secretory pathway: 1) *pep7* mutants showed an abnormal vacuolar morphology; 2) *pep7* mutants accumulated membrane vesicles in the cytoplasm; 3) *pep7* mutants demonstrated both transport and sorting defects of various vacuolar hydrolases within 5 min of loss of function; and 4) Pep7p was found in both a soluble fraction and a particulate fraction consistent with a post-Golgi complex, prevacuolar compartment.

The observation that *pep7* mutants contain a single large vacuolar compartment and wild-type yeast cells normally contain three to five moderately sized vacuolar compartments suggests that Pep7p does impinge on vacuolar function (Figure 4), and in this way may affect the production of active CPY. Furthermore, the accumulation of a 40–60-nm vesicle population in *pep7* mutants further suggests that this defect is in vesicle-mediated transport (Figure 5). Previous work on transport through the secretory pathway and the vacuolar branch of this pathway demonstrates that a block at a vesicle consumption step in these pathways can lead to the accumulation of vesicle populations of this size (Novick *et al.*, 1981; Newman and Ferro-Novick, 1987; Shim *et al.*, 1991; Cowles *et al.*, 1994; Piper *et al.*, 1994; Becherer *et al.*, 1996). Indeed, in many cases, vesicles in the size range of 30–60 nm have been demonstrated to be transport vesicles between organelle compartments in these pathways (reviewed in Ferro-Novick and Jahn, 1994; Rothman, 1994). These accumulated vesicles are significantly smaller than the secretory vesicles that transport secreted proteins from the yeast TGN to the plasma membrane; these secretory vesicles measure approximately 100 nm in diameter (Novick *et al.*, 1981). Therefore, the 40–60-nm vesicles seen in *pep7* mutants are not likely to be plasma membrane-targeted secretory vesicles. Furthermore, the defect in *pep7* mutants does not appear to involve any step in the ER/Golgi complex/plasma membrane portion of the secretory pathway because synthesis of secreted enzyme invertase is not affected in these mutants (Garlow, 1989). Furthermore, the loss of Pep7p function leads to a block in synthesis of vacuolar hydrolases at points where they have received both ER and Golgi complex posttranslational modifications (Figures 6–8). Thus, the vesicles that accumulate in *pep7* mutants likely originate from the vacuolar branch of the secretory pathway. These observations indicate that Pep7p may function in vesicle-mediated transport somewhere between the yeast TGN and the yeast vacuole.

Analysis of vacuolar hydrolase synthesis in *pep7Δ* and *pep7–20* allele containing strains demonstrated that *pep7* mutants are indeed defective in transport not only of the CPY precursor to the vacuole but also of precursors to PrA and PrB. In *pep7* mutants, these three hydrolases are found in forms consistent with proper transport through the ER and Golgi complex, but not with transport to the vacuole where the final processing steps take place to produce active hydrolases of the mature size (Figures 6 and 8). The lack of processing of Golgi forms of CPY, PrA, and PrB is truly indicative of a transport defect and not an initial defect in processing, because in *pep7–20* mutants at the restrictive temperature the precursors to CPY, PrA, and PrB are not processed, whereas the ALP precursor is properly processed (see below). The processing of CPY, PrA, PrB, and ALP are all dependent on active PrA and are thought to occur at the same site near to or upon delivery to the vacuole (reviewed in Klionsky *et al.*, 1990; Jones and Murdock, 1994). Thus, the ALP precursor reaches the vacuole at the restrictive tem-

perature, whereas the CPY, PrA, and PrB precursors do not.

Although CPY, PrA, and PrB are all blocked in transport to the vacuole, the consequences of this blockage differ for these hydrolases. The vast majority of Golgi form CPY is secreted at the cell surface, whereas the Golgi forms of PrA and PrB are predominantly held in the cells but not delivered to the vacuole (Figures 6 and 8). The basis for this difference in behavior is not known but has been observed in other vacuolar pathway mutants (Robinson *et al.*, 1988; Becherer *et al.*, 1996). The observation that CPY is rapidly secreted at the plasma membrane again indicates that the secretory pathway leading to the plasma membrane is intact and unperturbed in *pep7* mutants. The small fraction of precursor CPY that accumulated internally in the *pep7–20* mutant at the restrictive temperature was not processed to the mature form upon incubation at the permissive temperature, suggesting that the accumulating compartment is not subsequently available for transport of CPY once, presumably, Pep7p function is restored. The origin of this nonproductive complex or compartment is unknown and awaits a detailed investigation of Pep7p function.

Localization studies presented here are also consistent with the above phenotypic observations. Pep7p was enriched in preparations that are thought to contain both vacuolar and endosomal membranes (Figure 13). Significantly, these preparations were not enriched for the TGN compartment, as seen by the lack of enrichment for TGN protein Kex2p (Figure 13). Fractionation by differential centrifugation indicated that Pep7p is not likely to be associated solely with the vacuole (Figure 14B), and therefore the enrichment seen in the vacuole/endosome preparation was likely to be due to endosomal association. We cannot, however, rule out the possibility that Pep7p is associated with transport vesicles that travel between the TGN and endosome. A portion of Pep7p was also found in the soluble fractions (Figure 14B), indicating that Pep7p may be found both as a soluble cytoplasmic protein and as an organelle-associated protein. Protease K protection assays indicate that all of the Pep7p is freely accessible to exogenously added proteases and therefore is not sequestered in the lumen of a cellular organelle (Figure 15A). This is consistent with the observation that Pep7p is not predicted to contain a signal sequence for entry into the secretory pathway. Salt and urea treatment of cell extracts indicate that the portion of Pep7p associated with cellular organelles is peripherally bound (Figure 15B). Again, this is consistent with the prediction that Pep7p does not contain transmembrane domains. Because Pep7p was found both as a soluble cytoplasmic protein and associated with a cellular organelle, it is possible that Pep7p cycles between these two pools in executing its function. This is thought to be a common characteristic of many of the proteins known to function in vesicle-mediated transport (reviewed in (Ferro-Novick and Jahn, 1994; Rothman, 1994).

The conclusion that Pep7p is involved in vesicle-mediated protein transport between the TGN and endosome is further supported by our recent isolation of *VPS45* and *PEP12* as high copy suppressors of *pep7–20* mutant phenotypes (Webb *et al.*, 1997). Vps45p is similar to Sec1p, whereas Pep12p is similar to syntaxins (Cowles *et al.*, 1994; Piper *et al.*, 1994; Becherer *et al.*, 1996). Because both of these proteins are thought to be SNARE complex components involved in TGN-derived transport vesicle docking and/or fusion at the endosome, these genetic interactions further suggest that Pep7p functions at this step of transport. Indeed, the phenotypes of *pep7*, *pep12*, and *vps45* mutants are very much alike and include an enlarged single vacuolar compartment that is neutral in pH, extensive secretion of P2CPY, and accumulation of 40–60-nm vesicles. These common characteristics in part have been used to classify these mutants as class D vacuolar mutants (Raymond *et al.*, 1992). Furthermore, work in the laboratory of S. Emr reveals that Pep7p and Pep12p may be found in a complex (Burd and Emr, personal communication). The above described observations indicate that Pep7p indeed functions in the vesicle docking or fusion step in vesicle-mediated transport to the endosome via SNARE complex interactions.

Using the α-factor internalization and degradation assays, the endocytic pathway can be dissected into two steps: the internalization event and subsequent transport of internalized material to the vacuole. Mutations in *PEP7* differentially affected these two endocytic events. The internalization of α-factor was not impaired but degradation of internalized pheromone was delayed, suggesting that transport of pheromone to the vacuole was slowed but not completely blocked (Figures 12 and 13). It should be noted that imposition of the conditional *pep7–20* block requires a 5-min incubation at 37°C. Because of experimental constraints, this preincubation was not possible in the α-factor internalization and degradation assay (see MATERIALS AND METHODS). Therefore, the partial block seen in α-factor degradation may underestimate the severity of the block because of a delay in imposition of the block upon transfer to 37°C. The assays of Lucifer yellow accumulation are consistent with an incomplete block in transport to the vacuole (Figure 10). There are several possibilities to explain these observations. First, Pep7p could act directly in the endocytic pathway, but there would be another protein that could partially substitute for its function. Second, there may be two alternative routes from an early endocytic compartment to the vacuole and the *pep7* mutation would only block one of these routes. In this case, one would have to postulate that α-factor

can only be transported by one of these routes. Finally, the major site of action of Pep7p may be in the vacuolar biosynthetic pathway before intersection with the endocytic pathway or in recycling of transport factors from the endocytic pathway. In this event, the result of the *pep7* mutation on the endocytic pathway would be indirect. Resolution of these possibilities would appear to await further development in defining pathway and compartment identity in vacuolar/endosomal transport.

As noted above in the discussion of hydrolase transport in a *pep7–20* conditional mutant, transport of Golgi forms of CPY, PrA, and PrB are blocked quickly after the loss of Pep7p function (Figure 8, A–C). The transport of ALP, however, is not immediately blocked (Figure 8D). In wild-type cells the precursor to ALP was initially thought to follow the same route to the vacuole as the precursor forms of CPY, PrA, and PrB (Klionsky *et al.*, 1990). Previous work on another vacuolar pathway mutant, the *vps1* mutant, indicated that in some mutants ALP can be routed from the TGN to the vacuole via the plasma membrane (Nothwehr *et al.*, 1995). Experiments with *pep7–20 end4Δ* double mutants indicate that the ALP precursor still reaches the vacuole when both the Pep7p-dependent route and the endocytic route are blocked. These data indicate that ALP does not reach the vacuole via endocytosis in the *pep7* mutant. Therefore, in wild-type cells at least two paths exist for transport of proteins from the TGN to the vacuole. One pathway is Pep7p-dependent and is responsible for transport of the precursors to CPY, PrA, and PrB, and the second pathway is Pep7p-independent and is responsible for transport of the precursor to ALP. This second Pep7p-independent pathway does not include transport to the plasma membrane followed by endocytosis, and therefore is likely to operate in parallel with the pathway taken by CPY, PrA, and PrB. While this work was ongoing the same phenomenon was observed in *vps15*, *vps34* (Herman *et al.*, 1991; Stack *et al.*, 1995), and *pep12* conditional mutants (Rieder and Emr, personal communication), suggesting that an entire set of proteins function exclusively on one of two pathways. It is not clear at this point whether the precursor to ALP is routed separately through the same endosomal compartment, a separate endosomal compartment, or does not include an endosomal compartment between the Golgi complex and the vacuole. Recent evidence from multiple steps in the secretory pathway indicate that parallel paths for transport of different cargo between cellular organelles may be common (reviewed in Bednarek *et al.*, 1995; Harsay and Bretscher, 1995; Schekman and Orci, 1996). Therefore, transport between the yeast TGN and endosome and/or vacuole may use not only similar components to carry out vesicle-mediated transport (SNARE components), but may also be structured similarly on a larger scale through the incorporation of parallel pathways.

It should be noted that although ALP is properly transported and processed in *pep7–20* mutants at the restrictive temperature (Figure 8D, lane 3), mutants carrying null alleles of *pep7* are unable to process precursor ALP (Figure 6, lane 3; Figure 8D, lane 5). Failure to process a vacuolar hydrolase precursor is usually taken to indicate that the precursor has not been delivered to the vacuole where this modification normally takes place. However, when the processing hydrolase itself (PrA) is present in an inactive form and/or not present in the vacuole, this inference is not valid. At permissive temperatures, the *pep7–20* strain demonstrates no defect in hydrolase transport or processing and therefore the vacuole is likely to contain a full complement of processing enzyme (Figure 8D, lane 3). It is reasonable to conclude that the vacuoles in these mutants will remain competent to carry out PrA-dependent processing for some finite amount of time following a shift to the restrictive temperature, despite the near immediate loss in the ability to transport newly synthesized processing enzyme (PrA) to the vacuole. This is in fact what we see with precursor ALP processing in the *pep7–20* mutant at the restrictive temperature (Figure 8B, lane 3). However, following growth for multiple generations without the ability to produce active processing enzyme, the cells should lose the ability to process even those hydrolases that can be delivered to the vacuole. We infer that this is what we observe in the strains deleted for *PEP7*. A similar phenomenon in the form of phenotypic lag has been observed previously for ALP synthesis (Zubenko *et al.*, 1982).

Previous work carried out on *PEP7* (designated *VAC1*) suggested that Pep7p functioned directly in the process of vacuolar inheritance during the cell cycle (Weisman and Wickner, 1992). The defect in sorting and transport of P2CPY is manifested within 5 min of transfer of the *pep7–20* mutant to 37°C (Figure 7C; Figure 8, lanes 3 and 4). If vacuolar inheritance were to be the primary defect, with sorting and processing defects secondary to the inheritance defect, the sorting and processing deficiency should only be seen near to or after the doubling time of the culture (more than 120 min in this regimen). This expectation is clearly at odds with the data. The results presented here indicate that a primary defect is transport to the endosome. This same phenomenon has been seen in several other class D vacuolar pathway mutants (Raymond *et al.*, 1992).

From the above discussed data, we propose the following working model for transport of yeast vacuolar hydrolases from the TGN (Figure 16). We postulate that Pep7p functions to facilitate the docking and/or fusion of a subset of TGN-derived transport vesicles at the endosome. This subset of vesicles trans-

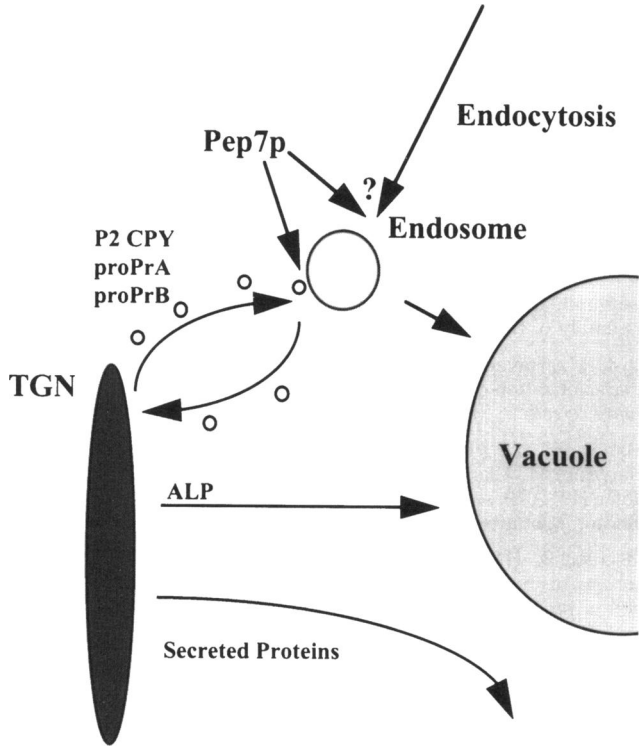

Figure 16. Proposed site of function of Pep7p. The presented observations of vesicle accumulation and hydrolase sorting/transport defects along with protein localization data indicate that Pep7p functions to dock and/or fuse TGN-derived transport vesicles onto the yeast endosome. These vesicles transport precursors to CPY, PrA, and PrB but not the precursor to ALP. The ALP precursor is transported to the vacuole by a separate pathway that does not include delivery to the plasma membrane followed by endocytosis. Data further indicate that *pep7* mutations perturb an internal portion of the endocytic pathway but are inconclusive as to the site and degree of involvement of Pep7p.

ports precursors to CPY, PrA, and PrB. A second set of transport vesicles transports the precursor to ALP and does not utilize Pep7p function. We consider it likely that Pep7p cycles on and off a complex at the endosomal membrane. The loss of Pep7p function results in the accumulation of transport vesicles in the cytoplasm. Because of the block in transport, the P2CPY-sorting apparatus becomes sequestered in the accumulated transport vesicles, and in this way is rendered unable to perform subsequent rounds of sorting, resulting in secretion of P2CPY. The block at this early step of transport leads secondarily to the coalescence of the downstream vacuolar compartment to form a single large vacuole by unknown mechanisms. Perhaps related to this coalescence event, the mutants lose the ability to partition vacuolar fragments to the developing bud. The ability of the vacuole to carry out the PrA-dependent processing of ALP is eventually lost because the remaining PrA activity is diluted out by cell division and by the lack of inheritance of vacuolar material by newly formed cells.

Concomitantly with these changes, the loss of Pep7p function leads either primarily or secondarily to a block in transport of receptor-mediated endocytosed macromolecules at an internal compartment or vesicle population. It is not clear at this point if this endocytic pathway perturbation is in docking/fusing at the endosome, as indicated above, or a separate transport step.

ACKNOWLEDGMENTS

We thank Dr. Joseph Suhan for his assistance with electron microscopy work and members of the Jones laboratory for their helpful discussions throughout the course of this work. This work was supported by grants from the National Institutes of Health (GM-29713 to E.W.J), the Swiss National Science Foundation, and the Kanton Basal Stadt (to H.R.). Computer analysis was carried out through the Pittsburgh Supercomputing Center grant IP41 RR06009. The Center for Light Microscope Imaging and Biotechnology is a Science and Technology Center of the National Science Foundation whose support (MCB-8920118) is acknowledged.

REFERENCES

Ausubel, F.M., Brent, R., Kingston, B.E., Moore, D.D., Smith, J.A., Seidman, J.G., and Struhl, K. (1987). Current Protocols in Molecular Biology, New York: Wiley Interscience.

Banfield, D.K., Lewis, M.J., and Pelham, H.R. (1995). A SNARE-like protein required for traffic through the Golgi complex. Nature *375*, 806–809.

Bankaitis, V.A., Johnson, L.M., and Emr, S.D. (1986). Isolation of yeast mutants defective in protein targeting to the vacuole. Proc. Natl. Acad. Sci. USA *83*, 9075–9079.

Banta, L.M., Robinson, J.S., Klionsky, D.J., and Emr, S.D. (1988). Organelle assembly in yeast: characterization of yeast mutants defective in vacuolar biogenesis and protein sorting. J. Cell Biol. *107*, 1369–1383.

Becherer, K.A., Rieder, S.E., Emr, S.D., and Jones, E.W. (1996). Novel syntaxin homologue, Pep12p, required for the sorting of lumenal hydrolases to the lysosome-like vacuole in yeast. Mol. Biol. Cell *7*, 579–594.

Bednarek, S.Y., Ravazzola, M., Hosobuchi, M., Amherdt, M., Perrelet, A., Schekman, R., and Orci, L. (1995). COPI- and COPII-coated vesicles bud directly from the endoplasmic reticulum in yeast. Cell *83*, 1183–1196.

Berg, J.M. (1990). Zinc fingers and other metal-binding domains. Elements for interactions between macromolecules. J. Biol. Chem. *265*, 6513–6516.

Cowles, C.R., Emr, S.D., and Horazdovsky, B.F. (1994). Mutations in the *VPS45* gene, a SEC1 homologue, result in vacuolar protein sorting defects and accumulation of membrane vesicles. J. Cell Sci. *107*, 3449–3459.

Davis, N.G., Horecka, J.L., and Sprague, G.F., Jr. (1993). cis- and trans-acting functions required for endocytosis of the yeast pheromone receptors. J. Cell Biol. *122*, 53–65.

Dulic, V., Egerton, M., Elguindi, I., Raths, S., Singer, B., and Riezman, H. (1991). Yeast endocytosis assays. Methods Enzymol. *194*, 697–710.

Ferro-Novick, S., and Jahn, R. (1994). Vesicle fusion from yeast to man. Nature *370*, 191–193.

Garlow, S. (1989). Analysis of the *PEP7* Gene from the Yeast *Saccharomyces cerevisiae*. Ph.D. Thesis. Pittsburgh, PA: Carnegie Mellon University.

Gorlich, D., Kostka, S., Kraft, R., Dingwall, C., Laskey, R.A., Hartmann, E., and Prehn, S. (1995). Two different subunits of importin cooperate to recognize nuclear localization signals and bind them to the nuclear envelope. Curr. Biol. *5*, 383–392.

Graham, T.R., and Emr, S.D. (1991). Compartmental organization of Golgi-specific protein modification and vacuolar protein sorting events defined in a yeast sec18 (NSF) mutant. J. Cell Biol. *114*, 207–218.

Harsay, E., and Bretscher, A. (1995). Parallel secretory pathways to the cell surface in yeast. J. Cell Biol. *131*, 297–310.

Herman, P.K., Stack, J.H., and Emr, S.D. (1991). A genetic and structural analysis of the yeast Vps15 protein kinase: evidence for a direct role of Vps15p in vacuolar protein delivery. EMBO J. *10*, 4049–4060.

Hill, J., Donald, K.A., Griffiths, D.E., and Donald, G. (1991). DMSO-enhanced whole cell yeast transformation (published erratum appears in Nucleic Acids Res. *19*: 6688, 1991). Nucleic Acids Res *19*, 5791.

Hodges, R.S., Sodek, J., Smillie, L.B., and Jurasek, L. (1972). Tropomyosin: Amino acid sequence and coiled-coil structure. Cold Spring Harbor Symp. Quant. Biol. *37*, 299–310.

Hoffman, C.S., and Winston, F. (1987). A ten-minute DNA preparation from yeast efficiently releases autonomous plasmids for transformation of *Escherichia coli*. Gene *57*, 267–272.

Hu, J.C., O'Shea, E.K., Kim, P.S., Sauer, R.T., Kohn, W.D., Monera, O.D., Kay, C.M., and Hodges, R.S. (1990). Sequence requirements for coiled-coils: analysis with lambda repressor-GCN4 leucine zipper fusions. The effects of interhelical electrostatic repulsions between glutamic acid residues in controlling the dimerization and stability of two-stranded alpha-helical coiled-coils. Science *250*, 1400–1403.

Jones, E.W. (1977). Proteinase mutants of *Saccharomyces cerevisiae*. Genetics *85*, 23–33.

Jones, E.W. (1991a). Tackling the protease problem in *Saccharomyces cerevisiae*. Methods Enzymol. *194*, 428–453.

Jones, E.W. (1991b). Three proteolytic systems in the yeast *Saccharomyces cerevisiae*. J. Biol. Chem. *266*, 7963–7966.

Jones, E.W., and Murdock, D.G. (1994). Proteolysis in the yeast vacuole. In: Cellular Proteolytic Systems, ed. A.J. Ciechanover and A.L. Schwarts, New York: Wiley-Liss, 115–134.

Jones, E.W., Woolford, C.A., Moehle, C.M., Noble, J.A., and Innis, M.I. (1989). Genes, zymogens, and activation cascades of yeast vacuolar proteases. In: Cellular Proteases and Control Mechanisms: Proceedings of a Glaxo-UCLA Colloquium on Cellular Proteases and Control Mechansims, ed. T.E. Hugli, New York: Alan R. Liss, 141–147.

Jones, E.W., Zubenko, G.S., Parker, R.R., Hemmings, B.A., and Hasilik, A. (1981). Pleiotropic mutations of *S. cereivisiae* which cause deficiency for proteinases and other vacuole enzymes. In: Molecular Genetics in Yeast: Proceedings of the Alfred Benzon Symposium 16, ed. D. von Wettstein, J. Friis, M. Kielland-Brandt, and A. Stenderup, Copenhagen: Munksgaard, 182–198.

Kalinich, J.F., and Douglas, M.G. (1989). *In vitro* translocation through the yeast nuclear envelope. J. Biol. Chem. *264*, 17979–17989.

Klionsky, D.J., Banta, L.M., and Emr, S.D. (1988). Intracellular sorting and processing of a yeast vacuolar hydrolase: proteinase A propeptide contains vacuolar targeting information. Mol. Cell. Biol. *8*, 2105–2116.

Klionsky, D.J., and Emr, S.D. (1989). Membrane protein sorting: biosynthesis, transport and processing of yeast vacuolar alkaline phosphatase. EMBO J. *8*, 2241–50.

Klionsky, D.J., Herman, P.K., and Emr, S.D. (1990). The fungal vacuole: composition, function, and biogenesis. Microbiol. Rev. *54*, 266–292.

Kornfeld, S. (1987). Trafficking of lysosomal enzymes. FASEB J. *1*, 462–468.

Kornfeld, S., and Mellman, I. (1989). The biogenesis of lysosomes. Annu. Rev. Cell. Biol. *5*, 483–525.

Laemmli, U.K. (1970). Cleavage of structural proteins during the assembly of the head of bacteriophage T4. Nature *227*, 680–685.

Last, R.L., Stavenhagen, J.B., and Woolford, J.L. (1984). Isolation and characterization of the *RNA2*, *RNA3*, and *RNA11* genes of *Saccharomyces cerevisiae*. Mol. Cell. Biol. *4*, 2396–2405.

Manolson, M.F., Percy, J.M., Apps, D.K., Xie, X.S., Stone, D.K., Harrison, M., Clarke, D.J., and Poole, R.J. (1989). Evolution of vacuolar H+-ATPases: immunological relationships of the nucleotide-binding subunits. Biochem. Cell. Biol. *67*, 306–310.

Mechler, B., Hirsch, H.H., Muller, H., and Wolf, D.H. (1988). Biogenesis of the yeast lysosome (vacuole): biosynthesis and maturation of proteinase yscB. EMBO J. *7*, 1705–1710.

Moehle, C.M., Dixon, C.K., and Jones, E.W. (1989). Processing pathway for protease B of *Saccharomyces cerevisiae*. J. Cell Biol. *108*, 309–325.

Newman, A.P., and Ferro-Novick, S. (1987). Characterization of new mutants in the early part of the yeast secretory pathway isolated by a [3H]mannose suicide selection. J. Cell Biol. *105*, 1587–1594.

Nothwehr, S.F., Conibear, E., and Stevens, T.H. (1995). Golgi and vacuolar membrane proteins reach the vacuole in vps1 mutant yeast cells via the plasma membrane. J. Cell Biol. *129*, 35–46.

Novick, P., Ferro, S., and Schekman, R. (1981). Order of events in the yeast secretory pathway. Cell *25*, 461–469.

Piper, R.C., Cooper, A.A., Yang, H., and Stevens, T.H. (1995). VPS27 controls vacuolar and endocytic traffic through a prevacuolar compartment in *Saccharomyces cerevisiae*. J. Cell Biol. *131*, 603–617.

Piper, R.C., Whitters, E.A., and Stevens, T.H. (1994). Yeast Vps45p is a Sec1p-like protein required for the consumption of vacuole-targeted, post-Golgi transport vesicles. Eur. J. Cell Biol. *65*, 305–318.

Preston, R.A., Murphy, R.F., and Jones, E.W. (1989). Assay of vacuolar pH in yeast and identification of acidification-defective mutants. Proc. Natl. Acad. Sci. USA *86*, 7027–7031.

Preston, R.A., Reinagel, P.S., and Jones, E.W. (1992). Genes required for vacuolar acidity in *Saccharomyces cerevisiae*. Genetics *131*, 551–558.

Pryer, N.K., Wuestehube, L.J., and Schekman, R. (1992). Vesicle-mediated protein transport. Annu. Rev. Biochem. *61*, 471–516.

Raths, S., Rohrer, J., Crausaz, F., and Riezman, H. (1993). end3 and end4: two mutants defective in receptor-mediated and fluid-phase endocytosis in *Saccharomyces cerevisiae*. J. Cell Biol. *120*, 55–65.

Raymond, C.K., Howald-Stevenson, I., Vater, C.A., and Stevens, T.H. (1992). Morphological classification of the yeast vacuolar protein sorting mutants: evidence for a prevacuolar compartment in class E vps mutants. Mol. Biol. Cell *3*, 1389–1402.

Rieder, S.E., Banta, L.M., Kohrer, K., McCaffery, J.M., and Emr, S.D. (1996). Multilamellar endosome-like compartment accumulates in the yeast *vps28* vacuolar protein sorting mutant. Mol. Biol. Cell *7*, 985–999.

Riezman, H. (1993). Yeast endocytosis. Trends Cell Biol. *3*, 273–277.

Robbins, J., Dilworth, S.M., Laskey, R.A., and Dingwall, C. (1991). Two interdependent basic domains in nucleoplasmin nuclear targeting sequence: identification of a class of bipartite nuclear targeting sequence. Cell *64*, 615–623.

Robinson, J.S., Klionsky, D.J., Banta, L.M., and Emr, S.D. (1988). Protein sorting in *Saccharomyces cerevisiae*: isolation of mutants defective in the delivery and processing of multiple vacuolar hydrolases. Mol. Cell. Biol. *8*, 4936–4948.

Rose, M.D., and Fink, G.R. (1987). KAR1, a gene required for function of both intranuclear and extranuclear microtubules in yeast. Cell *48*, 1047–1060.

Rothblatt, J., and Schekman, R. (1989). Methods in cell biology: vesicular transport. In: A Hitchhiker's Guide to Analysis of the Secretory Pathway in Yeast, ed. A.M. Tartakoff, San Diego: Academic Press, 3–36.

Rothman, J.E. (1994). Mechanisms of intracellular protein transport. Nature *372*, 55–63.

Rothman, J.H., Howald, I., and Stevens, T.H. (1989). Characterization of genes required for protein sorting and vacuolar function in the yeast *Saccharomyces cerevisiae*. EMBO J. *8*, 2057–2065.

Rothman, J.H., and Stevens, T.H. (1986). Protein sorting in yeast: mutants defective in vacuole biogenesis mislocalize vacuolar proteins into the late secretory pathway. Cell *47*, 1041–1051.

Sambrook, J., Fritsch, E.F., and Maniatis, T. (1989). Molecular Cloning: A Laboratory Manual. Cold Spring Harbor, NY: Cold Spring Harbor Laboratory Press.

Schekman, R., and Orci, L. (1996). Coat proteins and vesicle budding. Science *271*, 1526–1533.

Schimmoller, F., and Riezman, H. (1993). Involvement of Ypt7p, a small GTPase, in traffic from late endosome to the vacuole in yeast. J. Cell Sci. *106*, 823–830.

Serrano, R. (1991). Transport across yeast vacuolar and plasma membrane. In: The Molecular and Cellular Biology of the Yeast *Saccharomyces*: Genome Dynamics, Protein Synthesis, and Energetics, ed. J.R. Broach, J.R. Pringle, and E.W. Jones, Plainview, NY: Cold Spring Harbor Laboratory Press, 523–585.

Sherman, F. (1991). Getting started with yeast. Methods Enzymol. *194*, 3–21.

Shim, J., Newman, A.P., and Ferro-Novick, S. (1991). The *BOS1* gene encodes an essential 27-kD putative membrane protein that is required for vesicular transport from the ER to the Golgi complex in yeast. J. Cell Biol. *113*, 55–64.

Singer, B., and Riezman, H. (1990). Detection of an intermediate compartment involved in transport of alpha-factor from the plasma membrane to the vacuole in yeast. J. Cell Biol. *110*, 1911–1922.

Singer-Kruger, B., Frank, R., Crausaz, F., and Riezman, H. (1993). Partial purification and characterization of early and late endosomes from yeast. Identification of four novel proteins. J. Biol. Chem. *268*, 14376–14386.

Stack, J.H., DeWald, D.B., Takegawa, K., and Emr, S.D. (1995). Vesicle-mediated protein transport: regulatory interactions between the Vps15 protein kinase and the Vps34 PtdIns 3- kinase essential for protein sorting to the vacuole in yeast. J. Cell Biol. *129*, 321–334.

Stevens, T., Esmon, B., and Schekman, R. (1982). Early stages in the yeast secretory pathway are required for transport of carboxypeptidase Y to the vacuole. Cell *30*, 439–448.

Van Den Hazel, H.B., Kielland-Brandt, M.C., and Winther, J.R. (1996). Review: biosynthesis and function of yeast vacuolar proteases. Yeast *12*, 1–16.

Vida, T.A., Huyer, G., and Emr, S.D. (1993). Yeast vacuolar proenzymes are sorted in the late Golgi complex and transported to the vacuole via a prevacuolar endosome-like compartment. J. Cell Biol. *121*, 1245–1256.

Webb, G.C., Hoedt, M., Poole, L.J., and Jones, E.W. (1997). Genetic interactions between *pep7* mutation and the *VPS45* and *PEP12* genes, which encode SNARE complex components of the vacuolar transport pathway in *Saccharomyces cerevisiae*. Genetics (*in press*).

Weisman, L.S., and Wickner, W. (1992). Molecular characterization of *VAC1*, a gene required for vacuole inheritance and vacuole protein sorting. J. Biol. Chem. *267*, 618–623.

White, T.J., Arnheim, N., and Erlich, H.A. (1989). The polymerase chain reaction. Trends Genet. *5*, 185–189.

Woolford, C.A., Dixon, C.K., Manolson, M.F., Wright, R., and Jones, E.W. (1990). Isolation and characterization of PEP5, a gene essential for vacuolar biogenesis in *Saccharomyces cerevisiae*. Genetics *125*, 739–752.

Yamamoto, A., DeWald, D.B., Boronenkov, I.V., Anderson, R.A., Emr, S.D., and Koshland, D. (1995). Novel PI(4)P 5-kinase homologue, Fab1p, essential for normal vacuole function and morphology in yeast. Mol. Biol. Cell *6*, 525–539.

Zubenko, G.S., Park, F.J., and Jones, E.W. (1982). Genetic properties of mutations at the *PEP4* locus in *Saccharomyces cerevisiae*. Genetics *102*, 679–690.